Hydrodynamic Simulations
- Physics, methods and codes -

- Radiation Hydrodynamic Simulations
- Simulation examples for Fast Ignition and high energy density physics

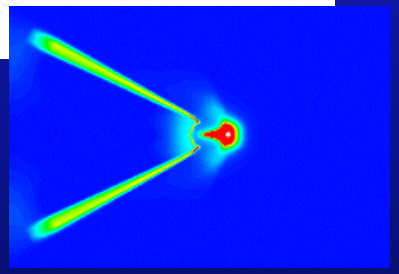

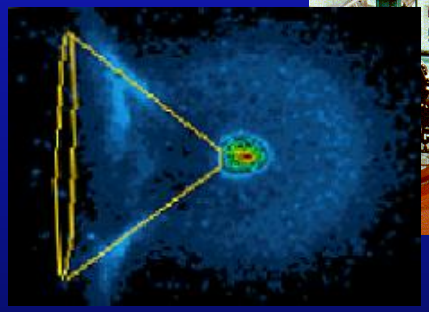

4th UK-Japan Winter School in High Energy Density Science
January 5, 2011, Edinburgh, The Royal Observatory

Institute of Laser Engineering, Osaka University
Hideo Nagatomo

2011/1/6

Contents

- Numerical method for radiation hydrodynamics
  - conservation, non-conservation
  - Arbitrary Lagrangian Eulerian method
- Recent computational simulations related to fast ignition
  - Radiation hydrodynamics
  - Fast ignition integrated interconnecting simulation system (FI^3)

density, temperature and pressure profiles of laser absorption and ablation

ILE Osaka

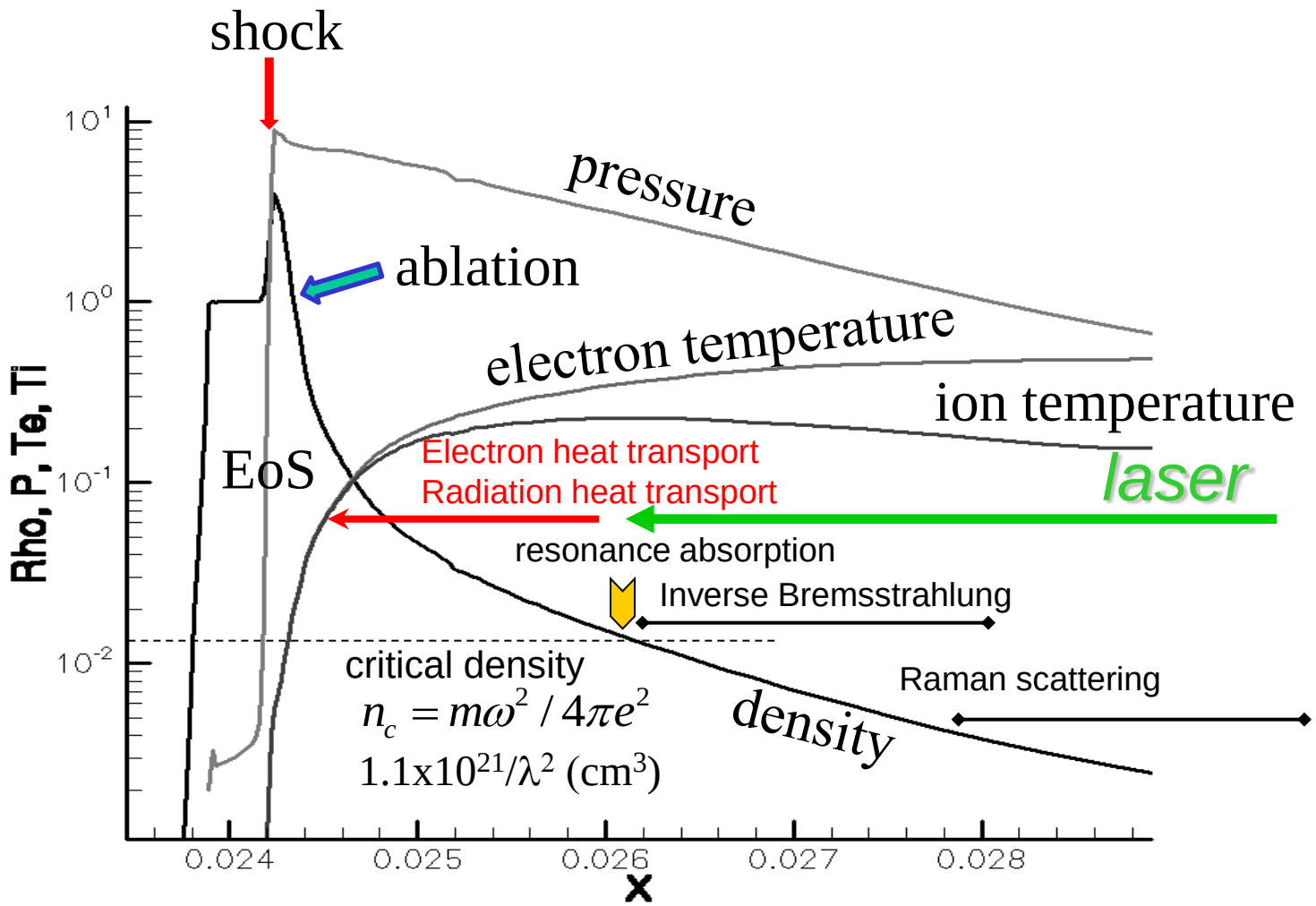

$$v_g \cdot \nabla I_L^k = -\nu_{abs} I_L^k \qquad S_L = \sum_k \nu_{abs} I_L^k / v_g^k$$

K. Mima, Laser Plasma Theory and Simulation, Harwood academic publishers, 1994.

Basic equation system of hydrodynamic

- **Mass**
- **Momentum**
- **Energy**
  - **electron energy**
  - **ion energy**
- **Thermal transport**
- **Radiation transport**
- **Equation of state**

$$e = \rho\left(\varepsilon + \frac{1}{2}u^2\right) \qquad p = (\gamma - 1)\varepsilon$$

- **Laser ray-tracing**
- **Laser absorption**

$$\frac{\partial \rho}{\partial t} + \frac{\partial (\rho u)}{\partial x} = 0$$

$$\frac{\mathrm{d}\rho}{\mathrm{d}t} = \frac{\partial \rho}{\partial t} + u\frac{\partial \rho}{\partial x} = -\rho\frac{\partial u}{\partial x}$$

$$\frac{\partial}{\partial t}(\rho u) + \frac{\partial}{\partial x}(\rho u^2 + p) = 0$$

$$\rho\frac{du}{dt} = \rho\left(\frac{\partial u}{\partial t} + u\frac{\partial u}{\partial x}\right) = -\frac{\partial p}{\partial x}$$

$$\frac{\partial}{\partial t}(e) + \frac{\partial}{\partial x}(eu + pu) = 0$$

$$\rho\frac{d\varepsilon}{dt} = \rho\left(\frac{\partial \varepsilon}{\partial t} + u\frac{\partial \varepsilon}{\partial x}\right) = -p\frac{\partial u}{\partial x}$$

non-conservation form

New ALE Method with CIP

ILE Osaka

1. Rezone the mesh for suitable shape
2. Obtain new value by solving the equation using CIP
   (Constrained Interpolation Profile ;Cubic-Interpolated Pseudo-Particles: Yabe *et. al.* JCP, 169, 556-593, 2001)

$$\frac{\partial f}{\partial t}+u\frac{\partial f}{\partial x}=0 \qquad \frac{\partial f'}{\partial t}+u\frac{\partial f'}{\partial x}=-f'\frac{\partial u}{\partial x}$$

$$f_i^{n+1}=a_i\xi^3+b_i\xi^2+c_i\xi+d_i \qquad \xi=-u\Delta t$$

$$f_i'^{n+1}=3a_i\xi^2+3b_i\xi+c_i$$

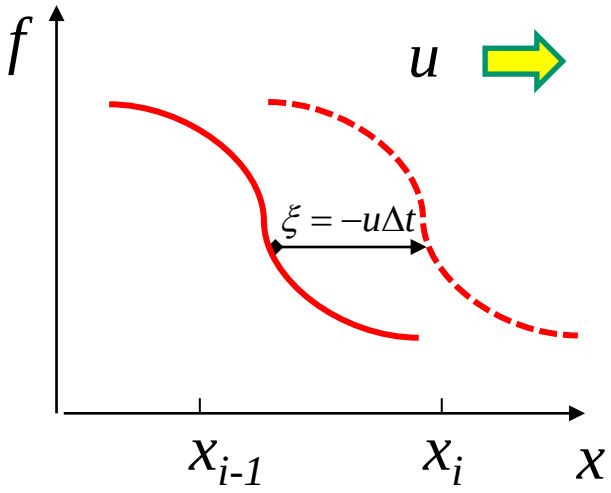

CIP method has high accuracy.
- ➔ Less dissipative.
- ➔ easy to make a code.
- ➔ Stable and robust. C-CUP, RCIP

ALE

$u=u_0-u_g$

rezoning; track mass center

Classical ALE and ALE-CIP method

ILE Osaka

1. solve the Lagrangian method
2. arrange the computational mesh (U_{ALE} is obtained)

$$\underbrace{\frac{\partial f}{\partial t}+U\frac{\partial f}{\partial x}}_{\frac{df}{dt}}+(U_{ALE}-U)\frac{\partial f}{\partial x}=0$$

f: valiable
U: fluid velocity
U_{ALE}: grid node velocity

cf. "An Arbitrary Lagrangian-Eulerian Computing Method for All Flow Speed", C.W. Hirt, A.A. Amsden, and J.L. Cook, JCP 14, 227-253 (1974).

1.grid velocity is included in CIP method.

$$\frac{\partial f}{\partial t}+U_{ALE}\frac{\partial f}{\partial x}=0$$

Conventional ALE and ALE-CIP

ILE Osaka

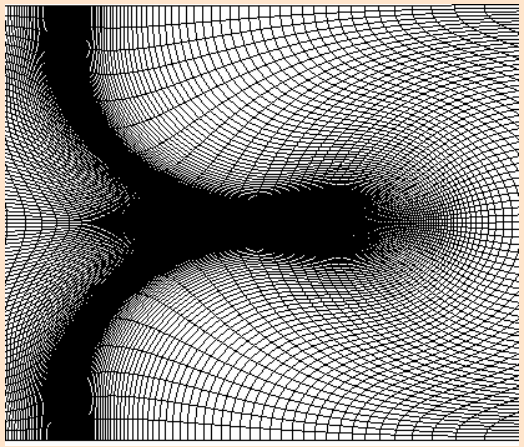

- difficulty of rezoning/ remapping in C-ALE
- difficulty of solving diffusion equations in C-ALE
- material tracking is easier.

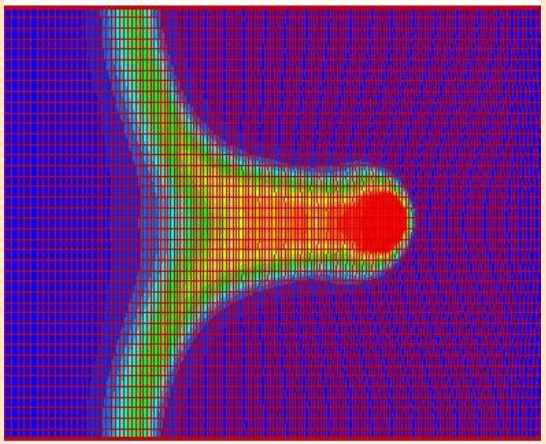

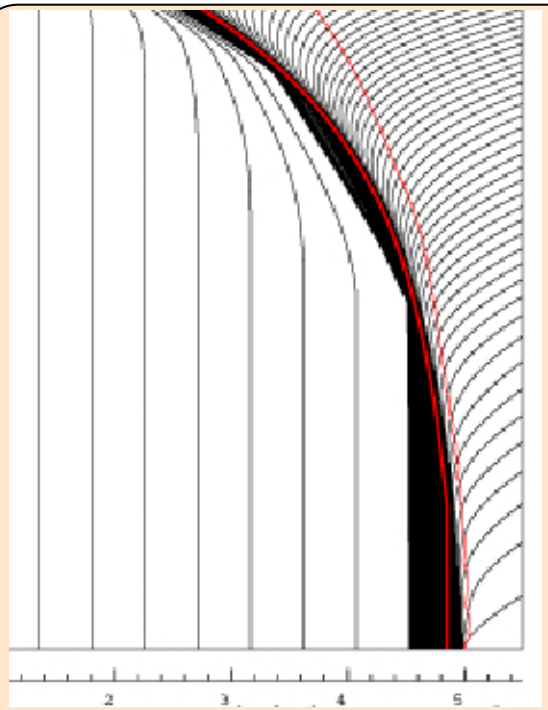

- rough computational mesh at laser absorption region in C-ALE.

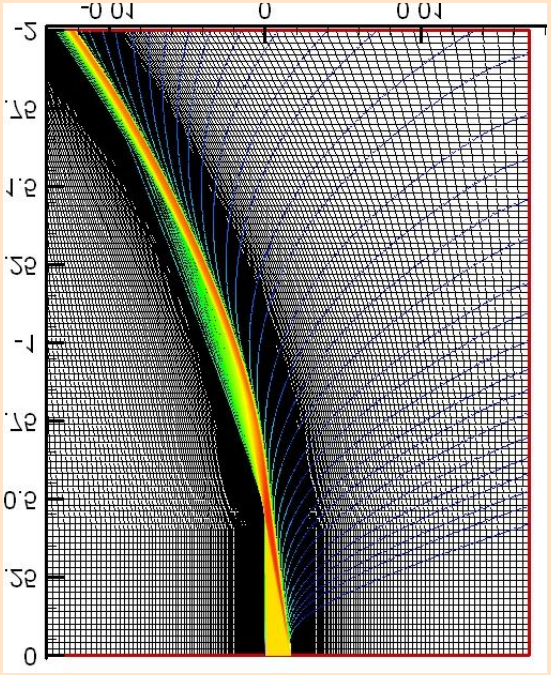

Electron heat conduction

ILE Osaka

energy density U
average velocity v_{av}
mean free path l

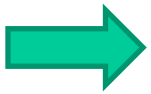

heat flux $q = -\dfrac{\mathrm{v}_{\mathrm{av}} l}{3} \nabla U$

$$\mathrm{v}_{\mathrm{av}} = \sqrt{k_b T_e / m}$$

$$l_{\mathrm{e}} = 1/(n_e \sigma_c) \propto T_e^2$$

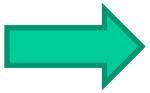

$$q = -\kappa_0 T_e^{5/2} \nabla T$$

diffusion approximation ; Spitzer-Härm (1962) thermal conductivity

$$\kappa_e = \kappa_0 T_e^{5/2} = (8/\pi)^{3/2} G(Z) \frac{(k_B T_e)^{5/2} k_B}{Z e^4 m_e^{1/2} \ln \Lambda}$$

Z dependance ; $G(Z) \approx (1 + 3.3/Z)$

Coulomb logarithms ; $\ln \Lambda$

heat transport

ILE Osaka

- Classical heat transport
  - diffusion approximation $q_{SH} \propto T_e^{5/2} \nabla T_e$
    Braginskii's thermal conductivity
  - flux limited diffusion $q_{effective}^{-1} = q_{SH}^{-1} + q_L^{-1} \quad q_L = f_L n_e v_e T_e$

- Kinetic effect
  (non-local heat transport)
  - Fokker-Planck equation

$$\frac{\partial f}{\partial t} + \mathbf{v} \cdot \nabla f - \frac{e(\mathbf{E} + \mathbf{V} \times \mathbf{B})}{m_e} = C(f) + H(f)$$

➔ Legendre polynomials

multi-group diffusion-type equations for radiation transport

frequency: ν intensity: I^{ν} emissivity: η^{ν} opacity: χ^{ν}

Fundamental equation for radiation transport (6-D Boltzmann equation）

$$\frac{1}{c}\frac{\partial I^{\nu}}{\partial t}+\Omega\bullet\nabla I^{\nu}=\eta^{\nu}-\chi^{\nu}I^{\nu}$$

Legendre expansion 0-th order momentum equation is ;

$$\frac{1}{c}\frac{\partial \mathrm{E}^{\nu}}{\partial \mathrm{t}}+\nabla\bullet\mathbf{F}^{\nu}=4\pi\eta^{\nu}-\chi^{\nu}cE^{\nu}$$

1st order momentum equation is ;

$$\frac{1}{c}\frac{\partial \mathbf{F}^{\nu}}{\partial \mathrm{t}}+c\nabla\bullet\mathbf{P}^{\nu}=-\chi^{\nu}c\mathbf{F}^{\nu}$$

under isotropic assumption, and c >> 1, finally ; $P^{\nu}=\frac{1}{3}E^{\nu}$ $\frac{c}{3}\nabla E^{\nu}=-\chi^{\nu}F^{\nu}$

$$\nabla\bullet\left(-\frac{c}{3\chi^{\nu}}\nabla E^{\nu}\right)=4\pi\eta^{\nu}-\chi^{\nu}cE^{\nu}$$

anisotropic case ; Eddington's factor f^{ν}

$$\mathbf{F}^{\nu}=-\frac{c}{\chi^{\nu}}\nabla\cdot(f^{\nu}E^{\nu})$$

D.M. Mihalas, *et al*, “Fundations of Radiation Hydrodynamics”, Oxford University Press, (1984).
G. Olson, *et al*., J. of Quantitative Spectroscopy & Radiative Transfer 64 (2000) 619-634

Fundamental equations of radiation hydrodynamics for laser plasma simulation

ILE Osaka

（1 fluid, 2 temperature plasma）

(mass)

$$\frac{d\rho}{dt} = -\rho \nabla \bullet \mathbf{u}$$

(momentum)

$$\rho \frac{d\mathbf{u}}{dt} = -\nabla P$$

(ion energy)

$$\rho \frac{d\varepsilon_i}{dt} = -P_i \nabla \cdot \mathbf{u} - \nabla \cdot q_i + Q_{ei}$$

(electron energy)

$$\rho \frac{d\varepsilon_e}{dt} = -P_e \nabla \cdot \mathbf{u} - \nabla \cdot q_e - Q_{ei} + S_L + S_r$$

(radiation transport)

$$\frac{1}{c}\frac{\partial I^{\nu}}{\partial t} + \Omega \cdot \nabla I^{\nu} = \eta^{\nu} - \chi^{\nu} I^{\nu} + S^{\nu}$$

(laser ray-trace and laser absorption)

$$v_g \cdot \nabla I_L^k = -\nu_{abs} I_L^k \qquad S_L = \sum_k \nu_{abs} I_L^k / v_g^k$$

PINOCO (2-D radiation hydrodynamic code)

- two temperature,
  - hydrodynamics
    - ALE-CIP （CIP, RCIP, CCUP）
- thermal transport (electron, ion)
  - flux limited type Spiter-Harm
  - implicit (9 points-ILUBCG)
- Radiation transport
  - multi-group diffusion type (16~64 groups)
  - implicit (9 points-ILUBCG)
  - Opacity, Emissivity
    - local thermodynamic equilibrium (LTE)
    - non-LTE, collisional radiative equilibrium (CRE)
- Equation of state
  - electron ; Tomas-Fermi model
  - ion ; Cowan model
- Laser ray-tracing
  - 1-D ray tracing
  - inverse-Bremsstrahlung absorption

Ablative R-T instability is one of the most critical issue for IFE

ILE Osaka

Target Laser

CH
Thickness 16 μm
Perturbation
wavelength 30μm
amplitude 0.5μm

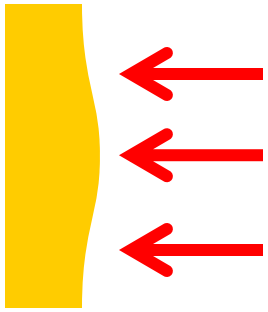

Intensity
7.0×10^{13} W/cm^2
Wave length
0.53mm

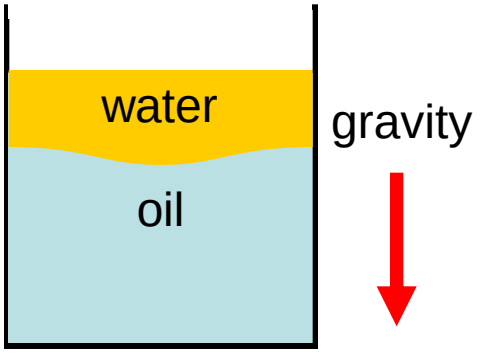

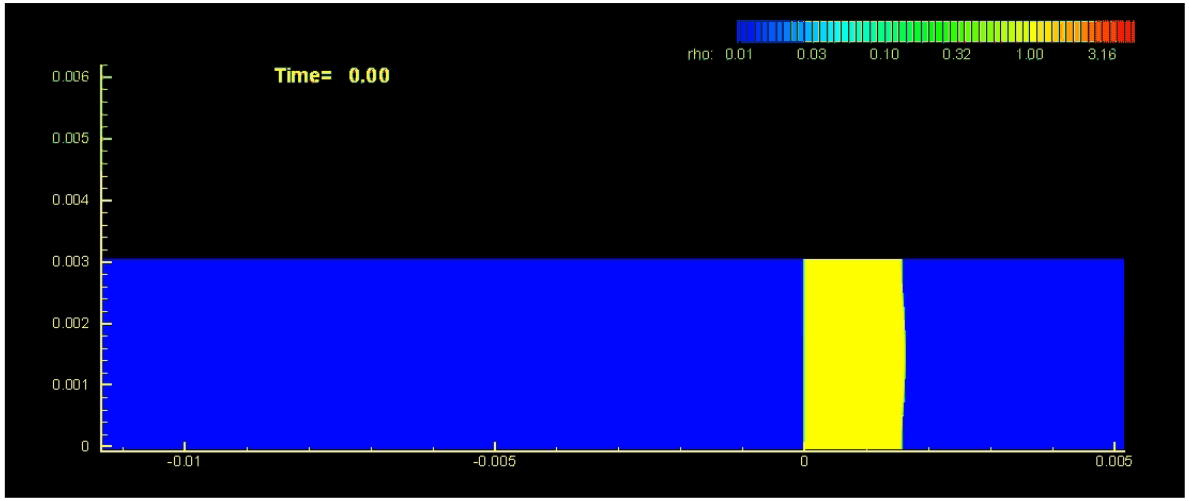

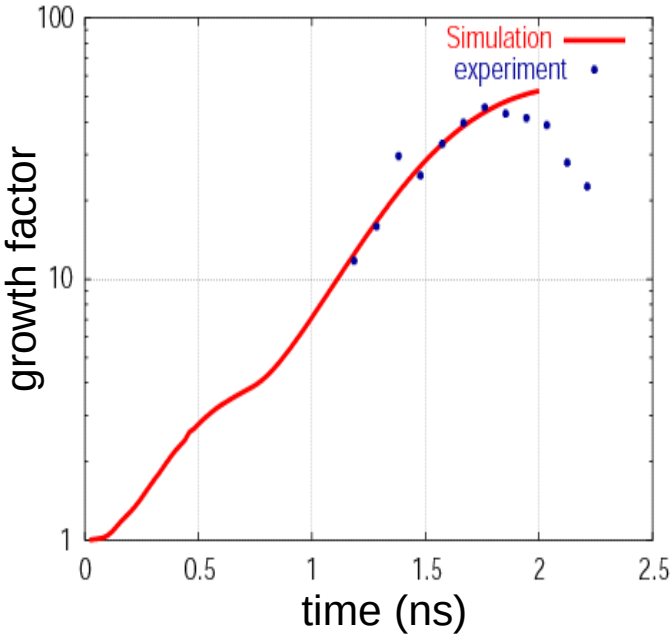

growth rate :

$$\gamma = \sqrt{\frac{kg}{1+kL}} - \beta k v_a$$

(Takabe, et al, Phys. Fluids, 26,2299 (1983)

Laser Fusion（Central Ignition, Indirect Drive）

ILE Osaka

Lawson condition;
1. High temperature (Ion temp.) T > 10^8K)
2. High density (ρ > 200g/cc)
3. High arial density(ρR > 0.3 g/cm^2)

Indirect drive (NIF, LMJ)

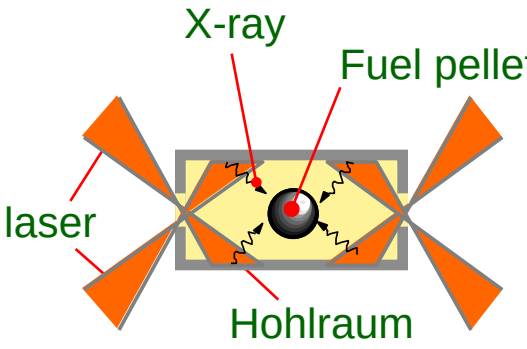

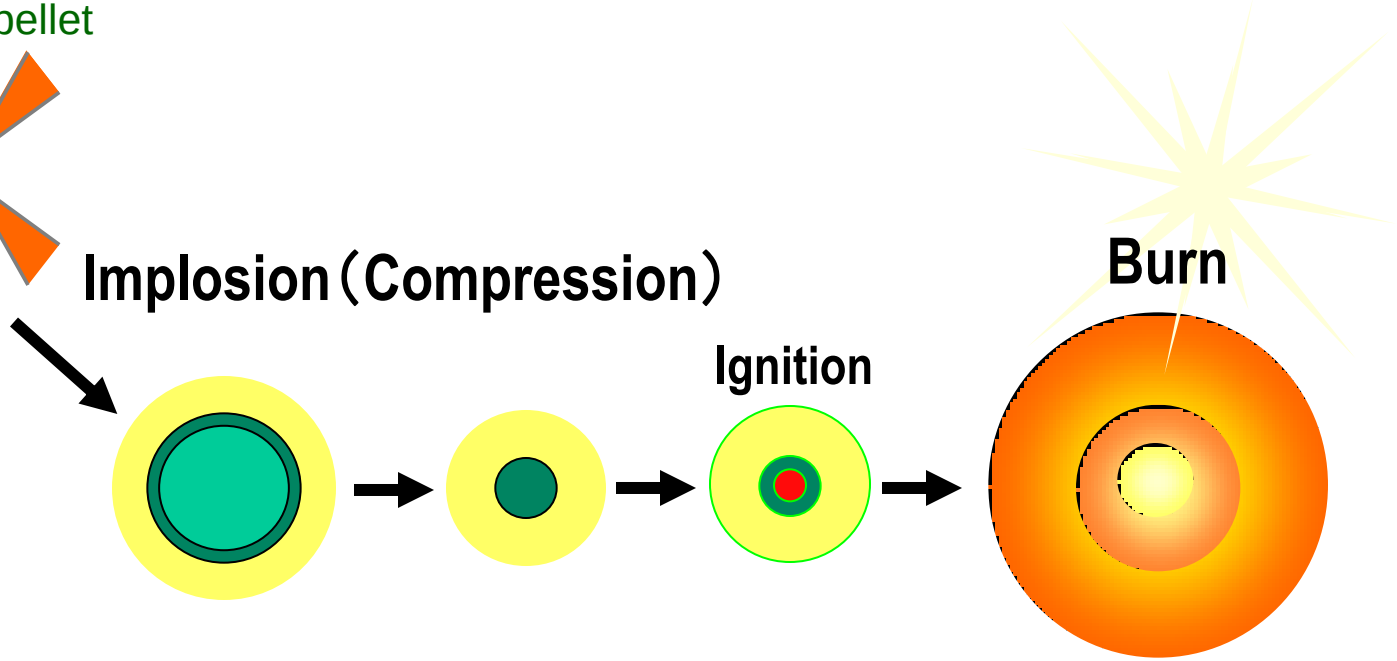

To suppress the R-T instability and other instabilities to achieve ignition, large laser facilities are required.

Gekko XII (Osaka, Japan, 1983)
25kJ, 0.53 μm, 12 beams
600 times of solid density

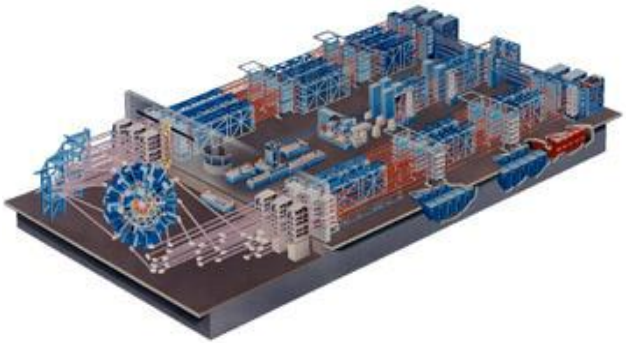

OMEGA (Rochester,USA)
30kJ, 0.35 μm, 60 beams
Gain of 0.01

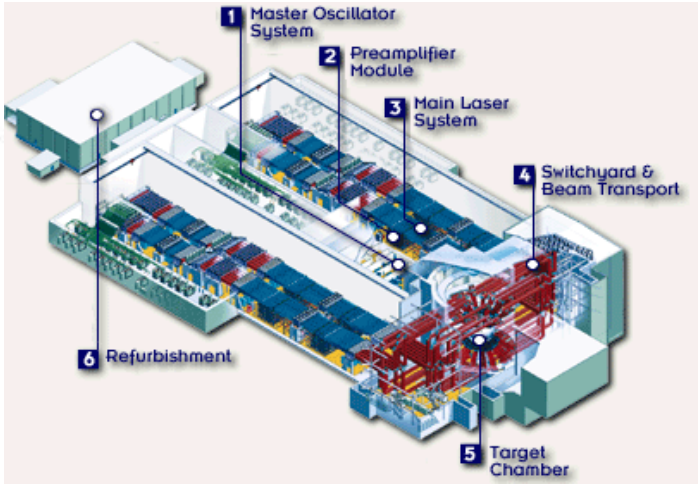

NIF; National Ignition Facility (LLNL, USA)
1.8MJ, 0.35 μm, 192 beams

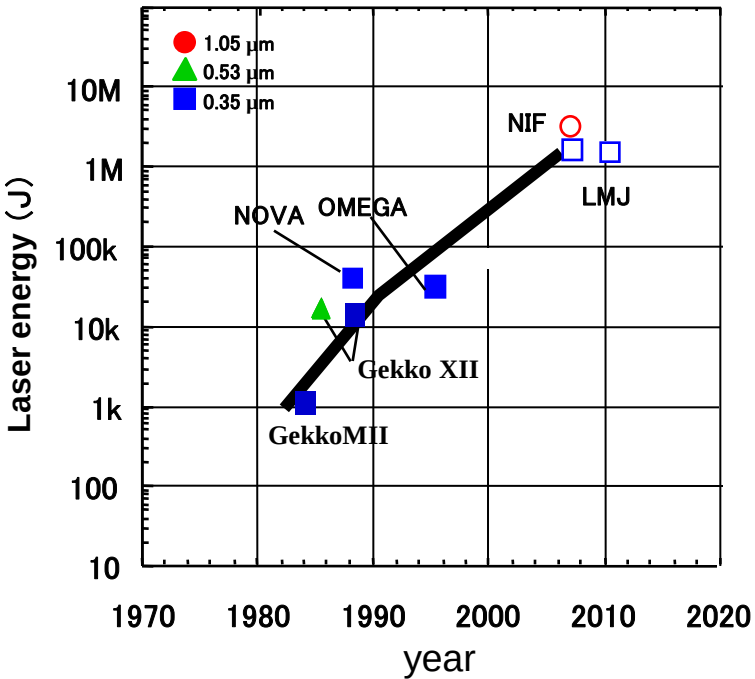

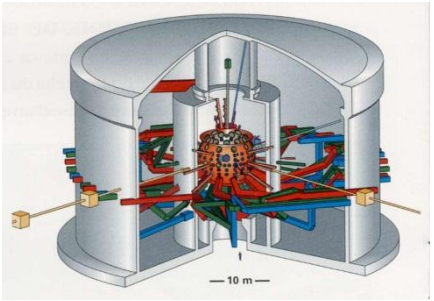

LMJ (Bordeaux, France)
1.8MJ, 0.35 μm, 192 beams

FIREX-I and GXII

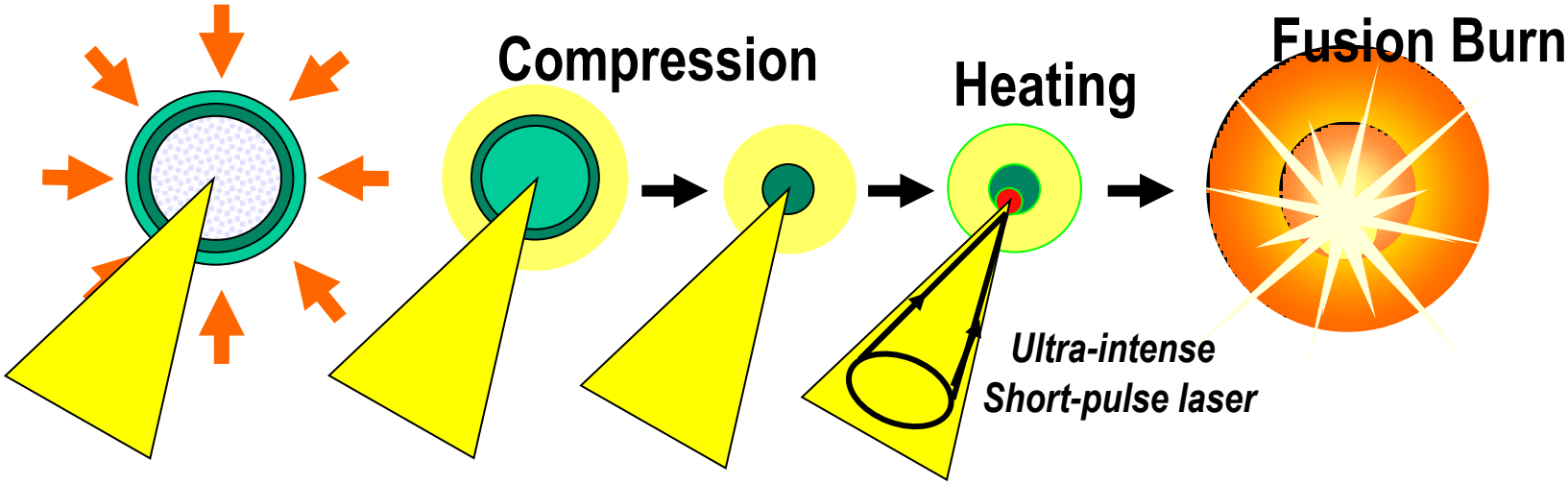

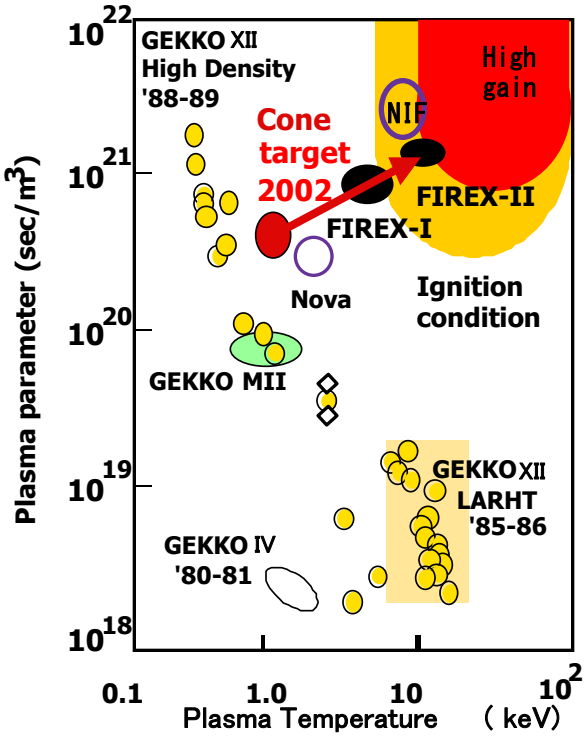

- In original FIREX-I design, implosion laser energy (GXII) is larger than the current condition.

FIREX-I

Implosion (GXII) ; 2.5~4.5 kJ in 2ω (Gaussian)

Heating (LFEX) ; 10 kJ in ω

Lasers for fusion and laser plasma research

ILE OSAKA

Peta watt Laser

1kJ/1ps

(1999-2006)

GXII

10kJ/1ns (1983-)

Target chamber I

(1983-)

LFEX Laser

2008- 10kJ/10ps

Target chamber II
HIPER

(1998-)

GMII (-2007)

By cone-guiding, heating laser can be introduced very near to the compressed core.

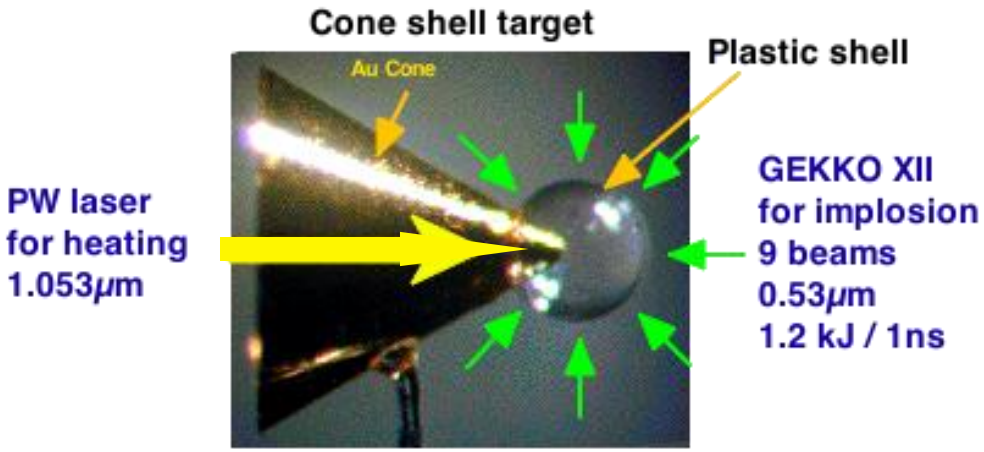

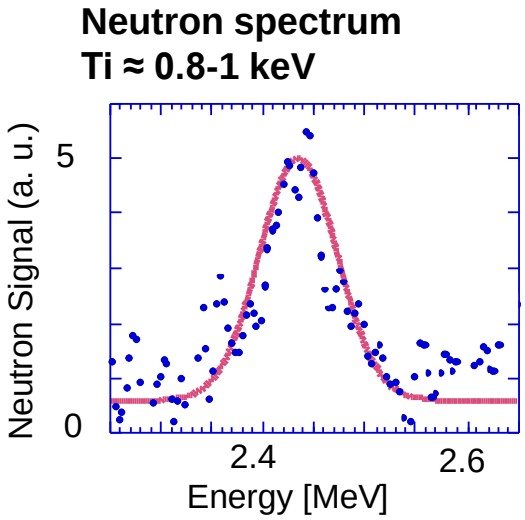

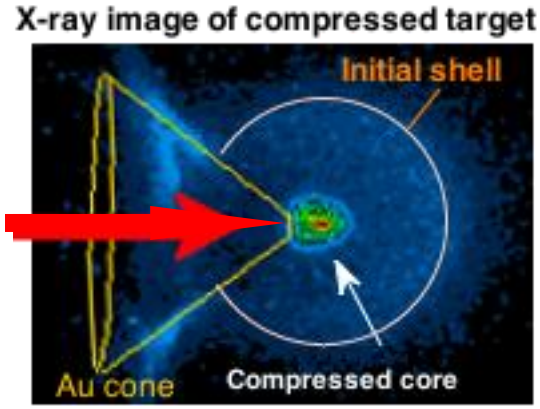

R. Kodama et al. Nature 2002.

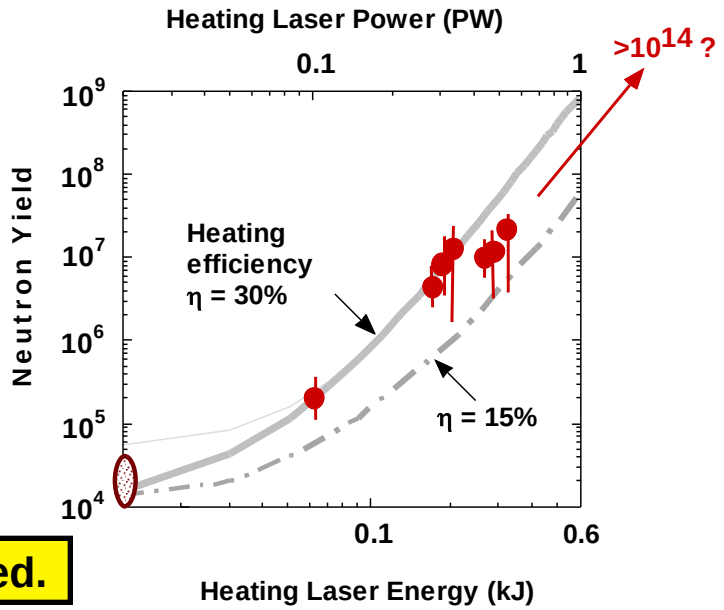

Efficient heating with | ~ 0.2 was demonstrated.

Numerical simulation of cone-guided implosion using 2D radiation-hydro simulation code “PINOCO”

ILE Osaka

Laser condition

Wavelength : 0.53mm

Energy : 3 kJ (Gaussian, on target, center focus)

PINOCO

- 2 temperature plasma
  - Hydro ALE-CIP method
- Thermal transport
  - flux limited type Spiter-Harm
  - Implicit (9 point-ILUBCG)
- Laser energy
  - 1-D ray-trace
- EOS
  - Tomas-Fermi
  - Cowan

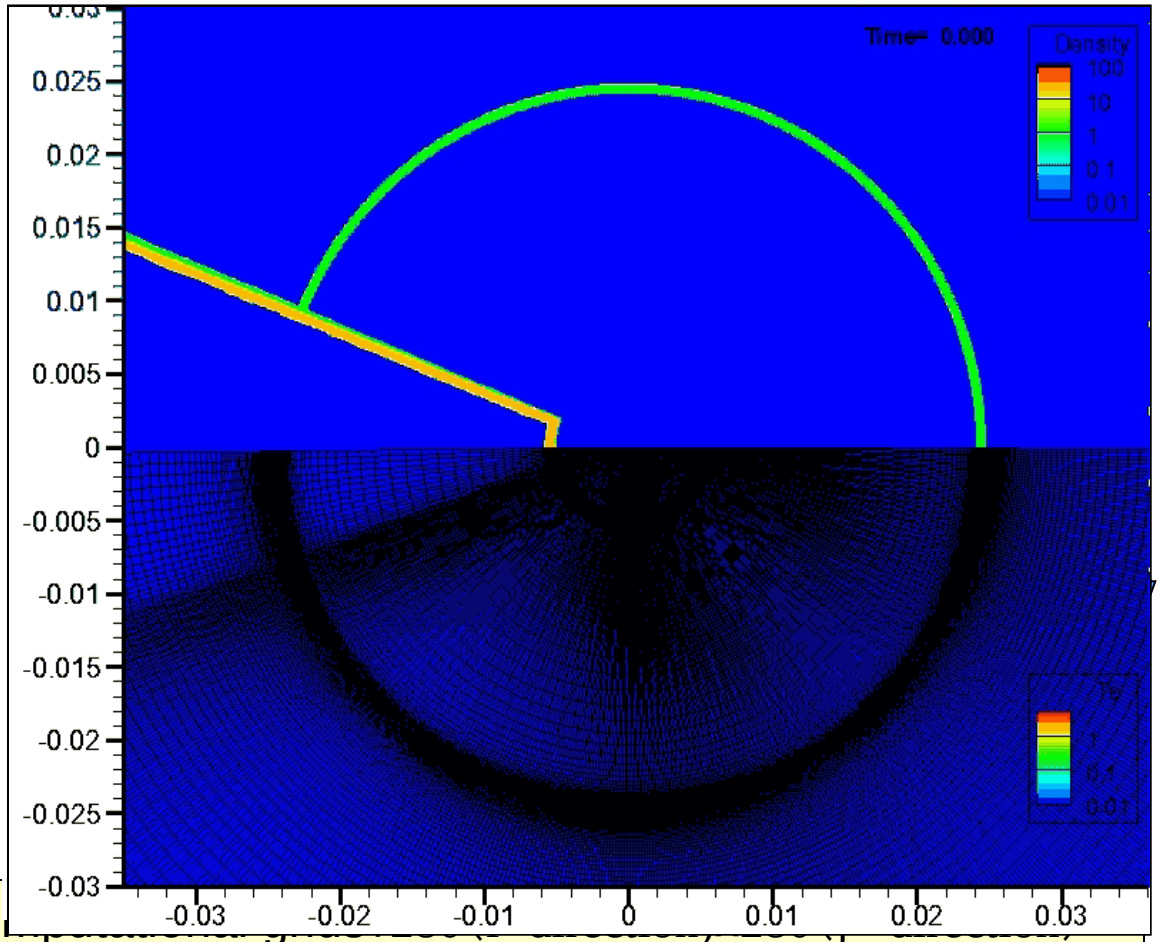

Example of Radiation hydrodynamic simulation;

Effect of radiation on the gold cone surface inside the shell in cone-guided shell implosion

Implosion Simulation

2-D implosion simulation of CH-D_2 shell with Au cone

Laser condition

Wavelength : 0.53mm

Energy : 3.5 kJ ((for 4π) Gaussian, FWHM=1.5ns)

Ray-trace : 1 - D (radial direction)

Radiation transport

Multi-group :

32 group and 16 group

(Two simulations to obtain numerical convergence in photon energy grid.)

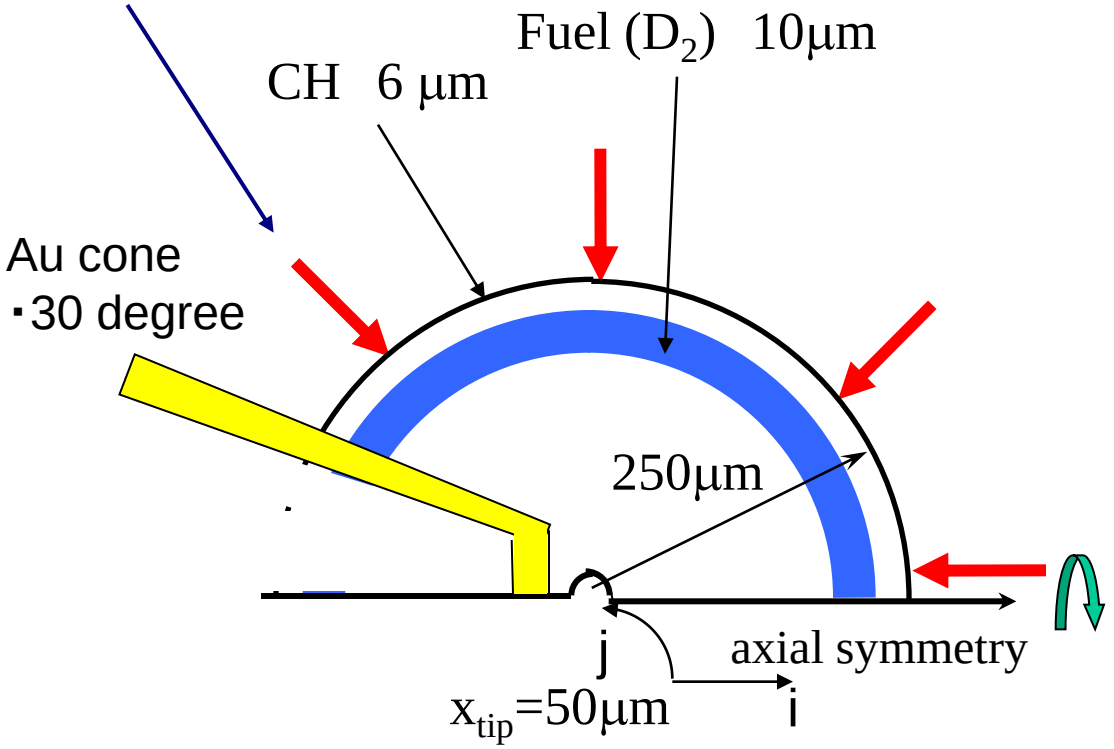

computational grids : 300 (i- direction) x 300 (j - direction)

Implosion Simulation

$CH\text{-}D_2$ shell + Au cone w/o coating

mass density contours (upper), and electron temperature (lower)

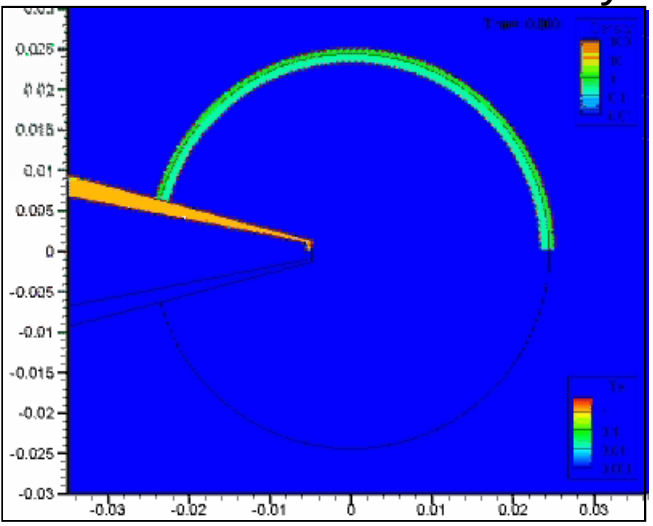

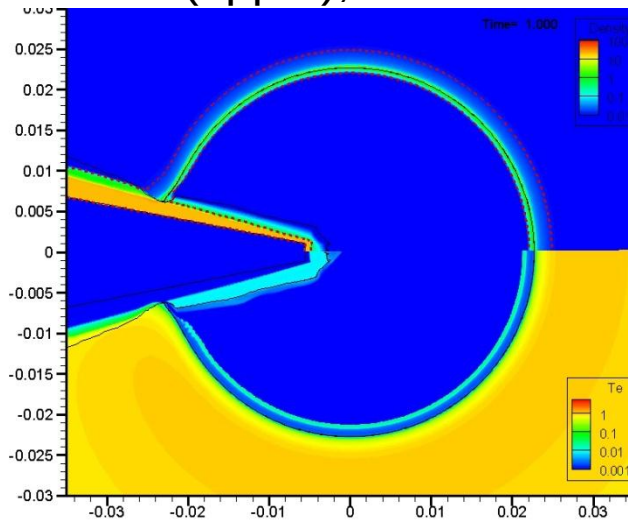

1.00 ns

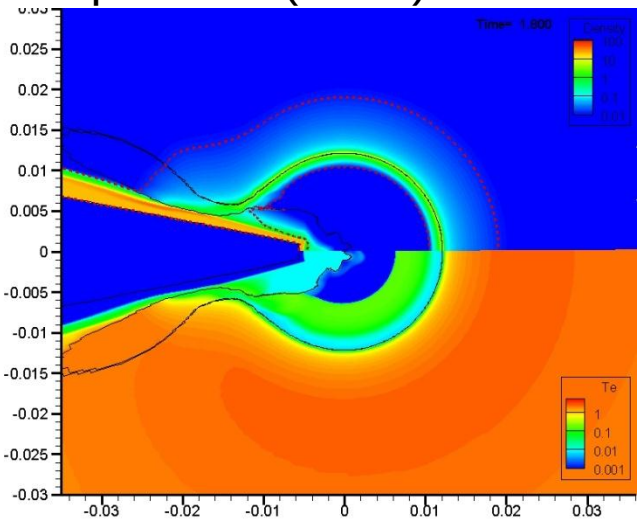

1.80 ns

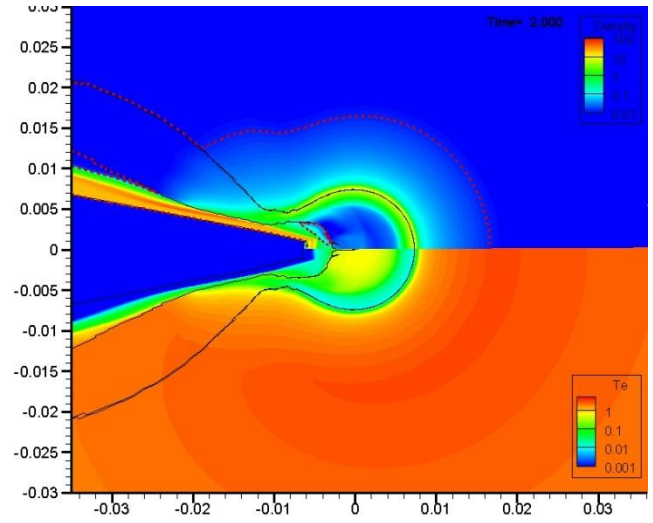

2.00 ns

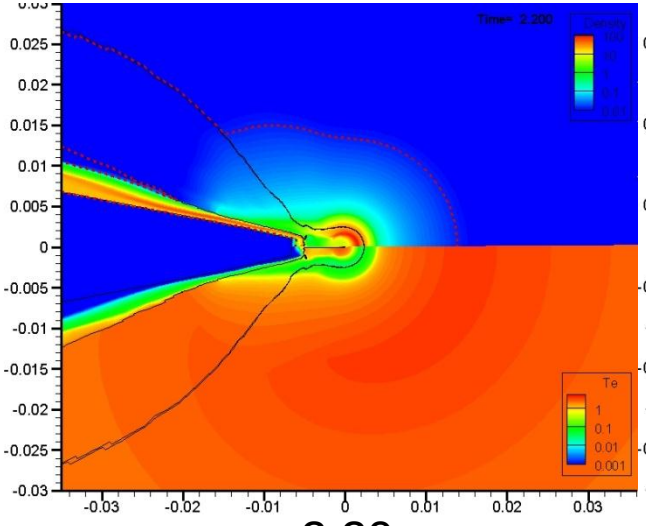

2.20 ns

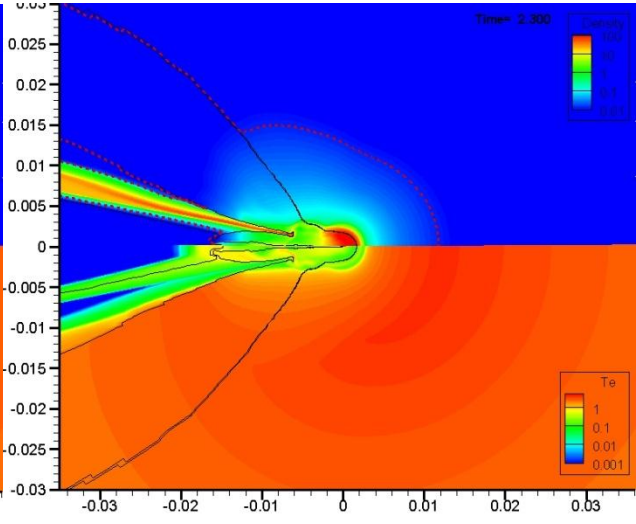

2.30 ns

Implosion Simulation

2-D implosion simulation of a CH-D_2 shell with Au coated cone

Laser condition

Wavelength : 0.53mm

Energy : 3.5 kJ ((for 4π) Gaussian, FWHM=1.5ns)

Ray-trace : 1 - D (radial direction)

Radiation transport

Multi-group :

32 group and 16 group

(Two simulations to obtain numerical convergence in photon energy grid.)

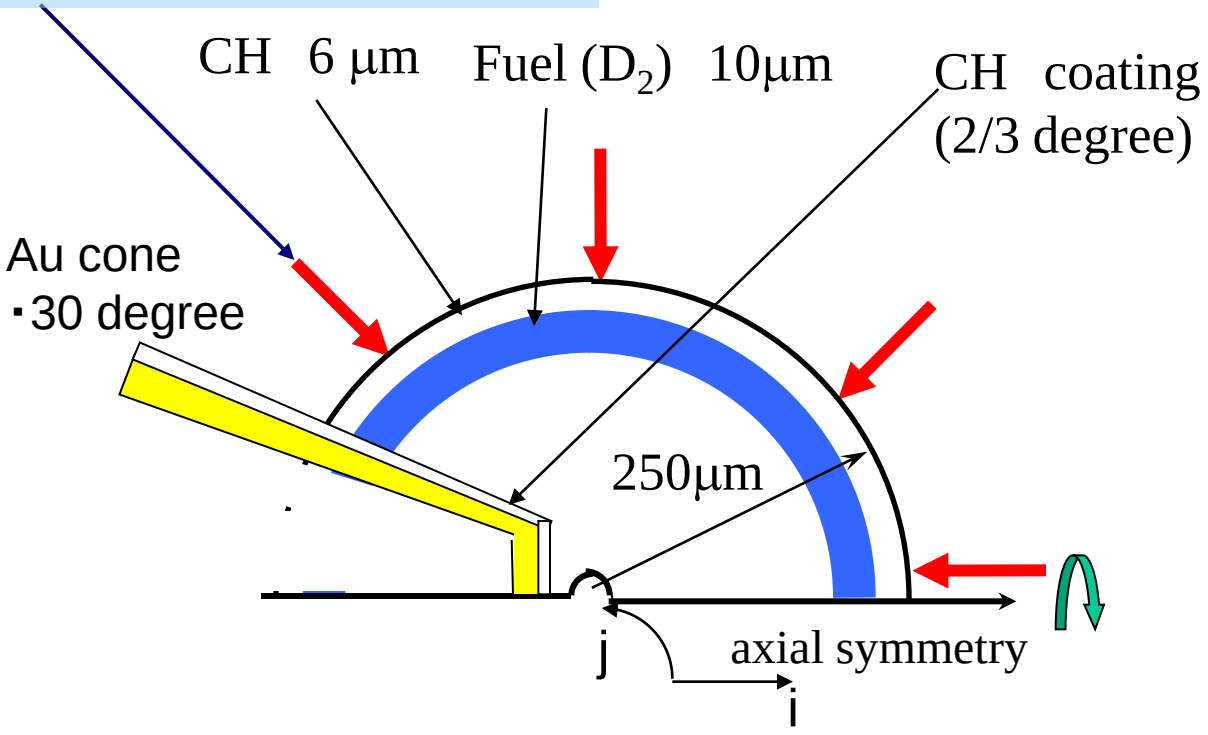

computational grids : 300 (i- direction) x 300 (j - direction)

Implosion Simulation

CH-D_2 shell +gold cone with CH coating

mass density contours (above), and electron temperature (below)

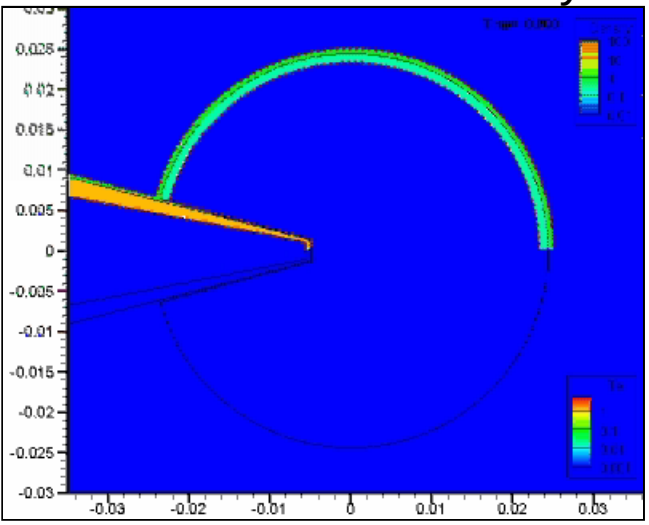

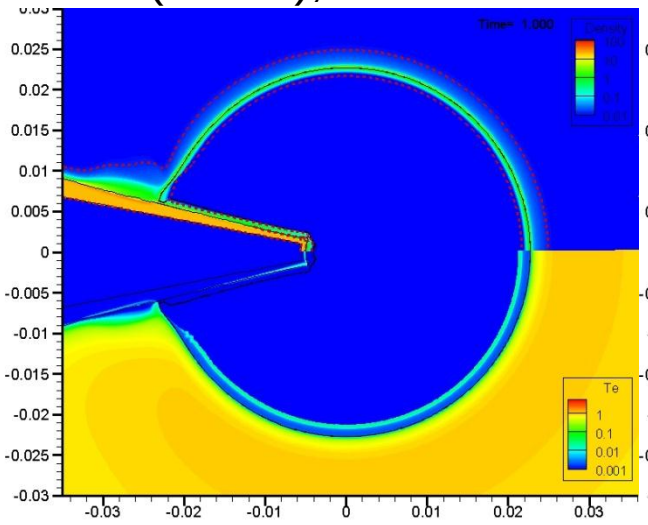

1.00 ns

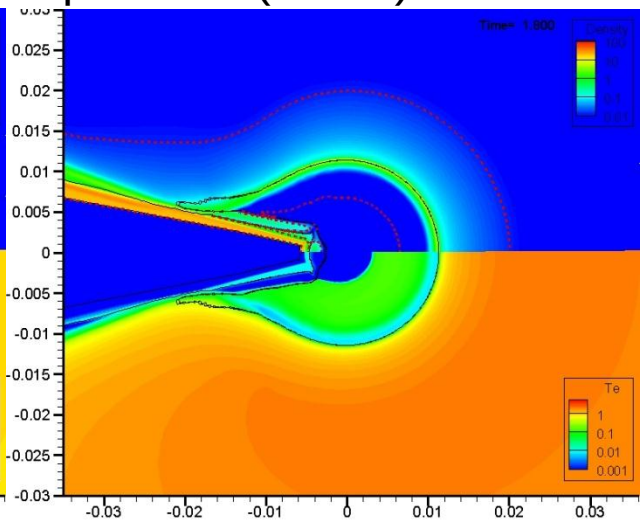

1.80 ns

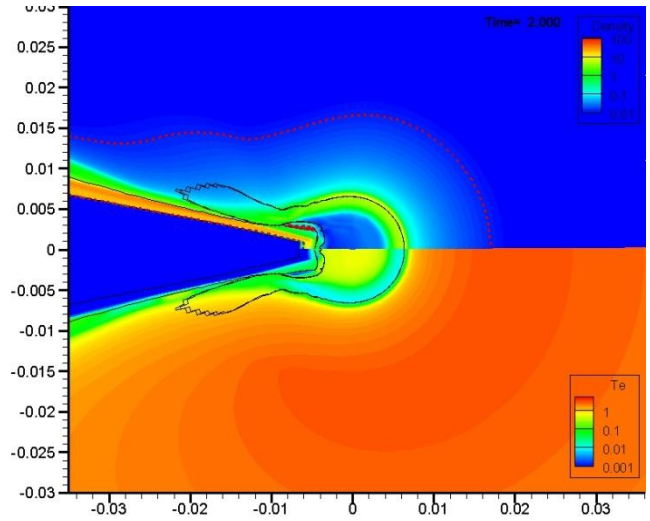

2.00 ns

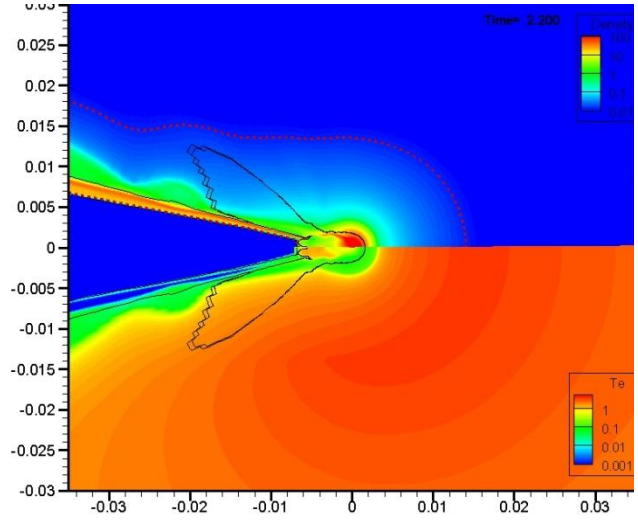

2.20 ns

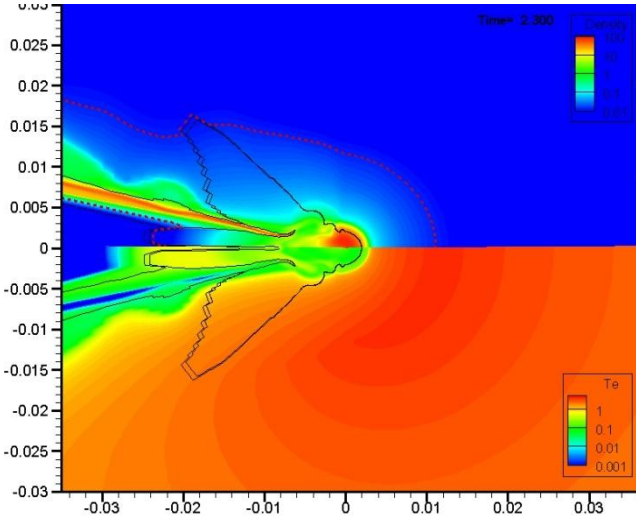

2.30 ns

Implosion Simulation

D_2 fuel is leaking near Au surface

D_2 fuel is leaking near Au surface in both cases. But it is less amount of leaking D_2 in case of with coating. This fact was not observed in a simulation without radiation transport.
Step at shell-cone interface may reduce the leaking. (R. B. Stephens, et al., PoP, **12**, 056312, 2005)

w/o coating

contact surface

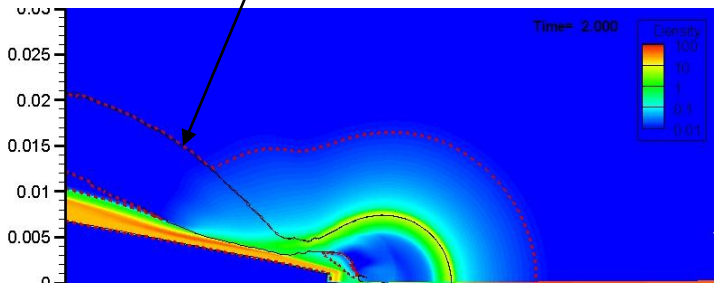

t=2.00 ns

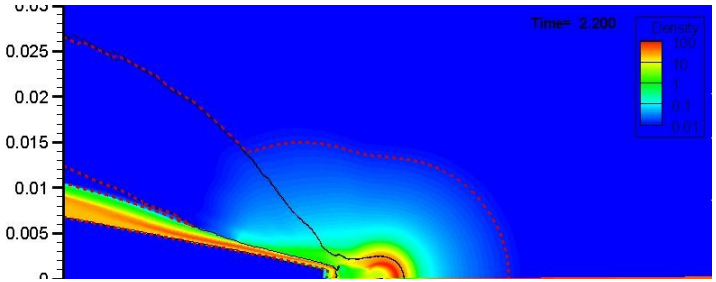

t=2.20 ns

with coating

contact surface

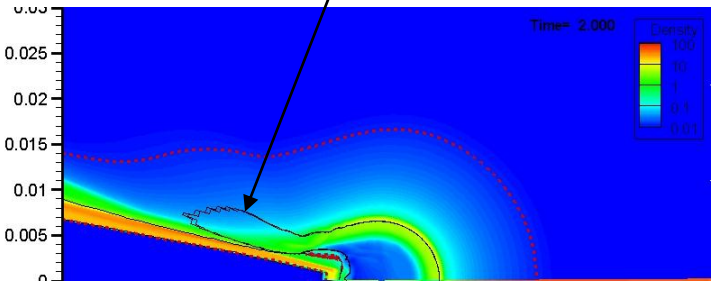

t=2.00 ns

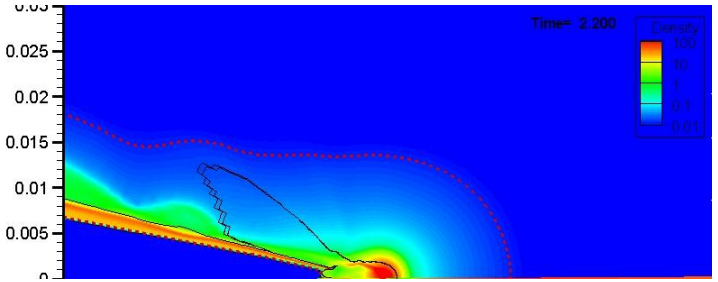

t=2.20 ns

Our previous work suggests that CH coating on the gold cone is effective to tamp ablated gold plasma which is expanding into the shell. (Nagatomo *et al*. PoP 2007)

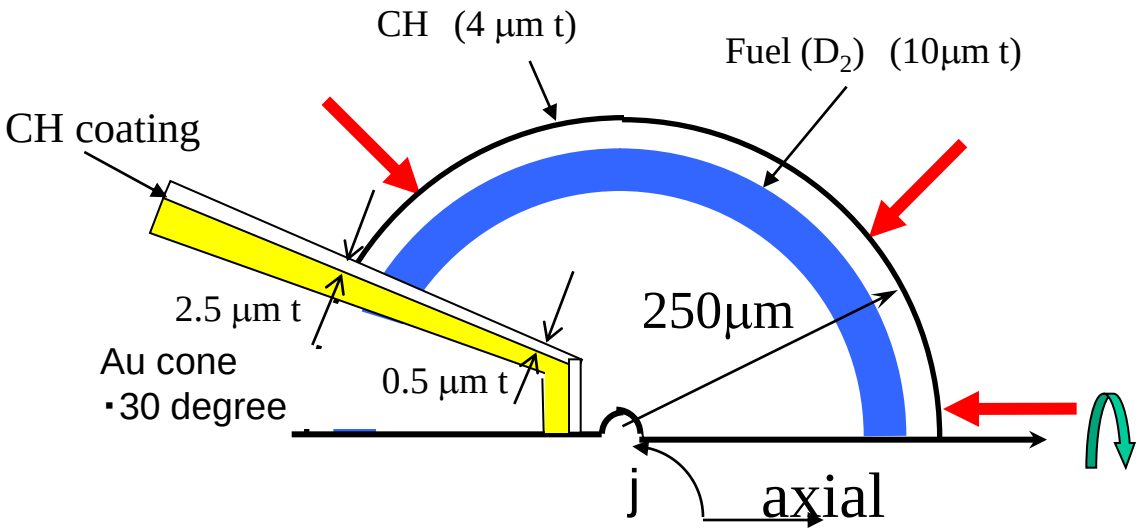

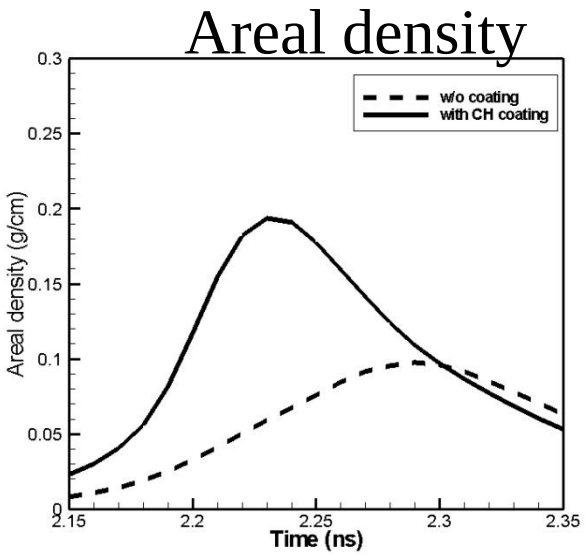

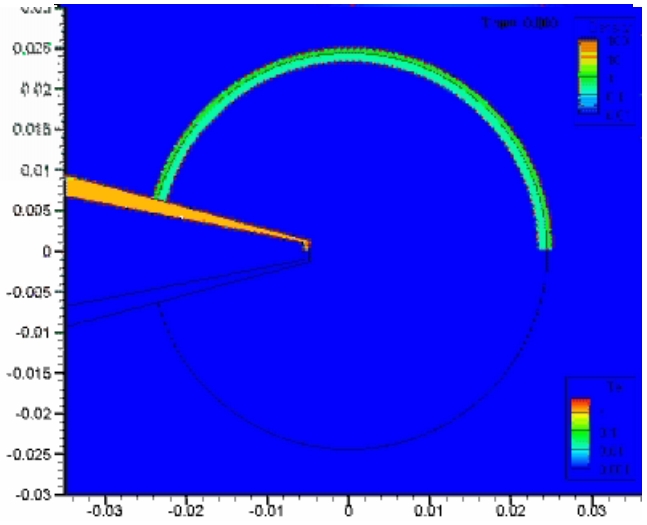

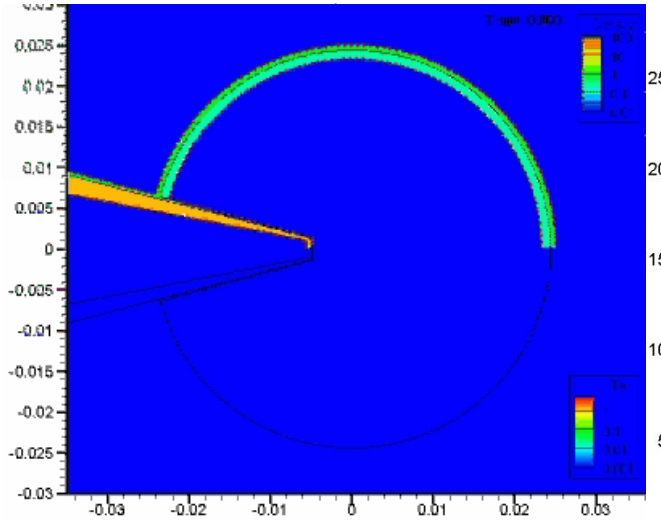

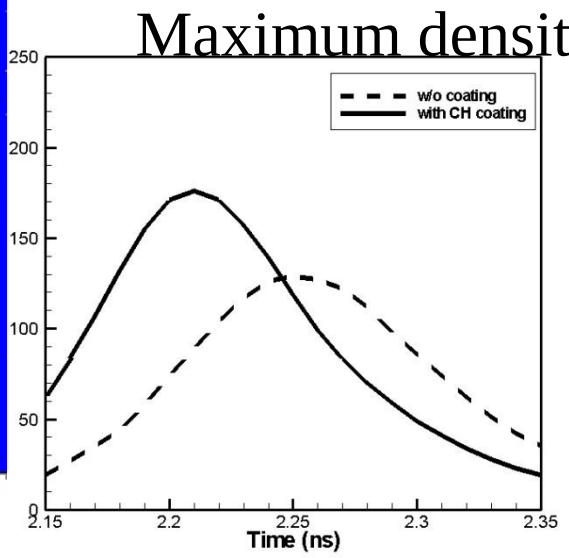

Example of Radiation hydrodynamic simulation;

Effect of Rayleigh-Taylor instability in cone-guided implosion.

1D simulation + perturbation models ; A standard target for GXII may be broken up before maximum compression

- ILESTA1D-FP
- + measured target surface roughness + Nakai-Azechi's imprint model

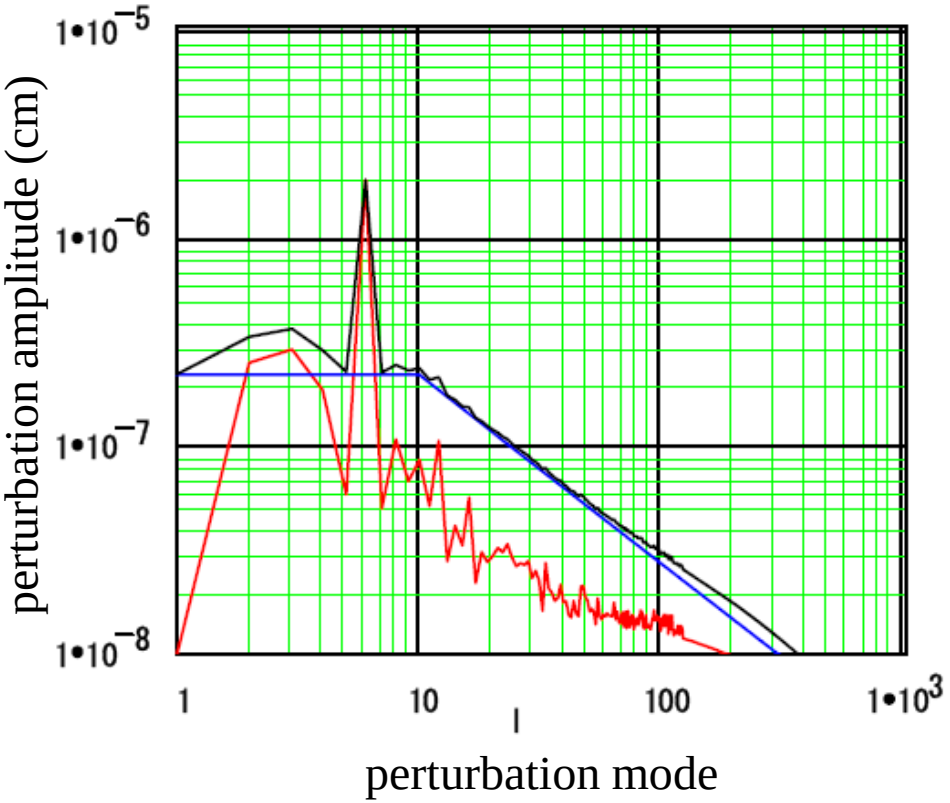

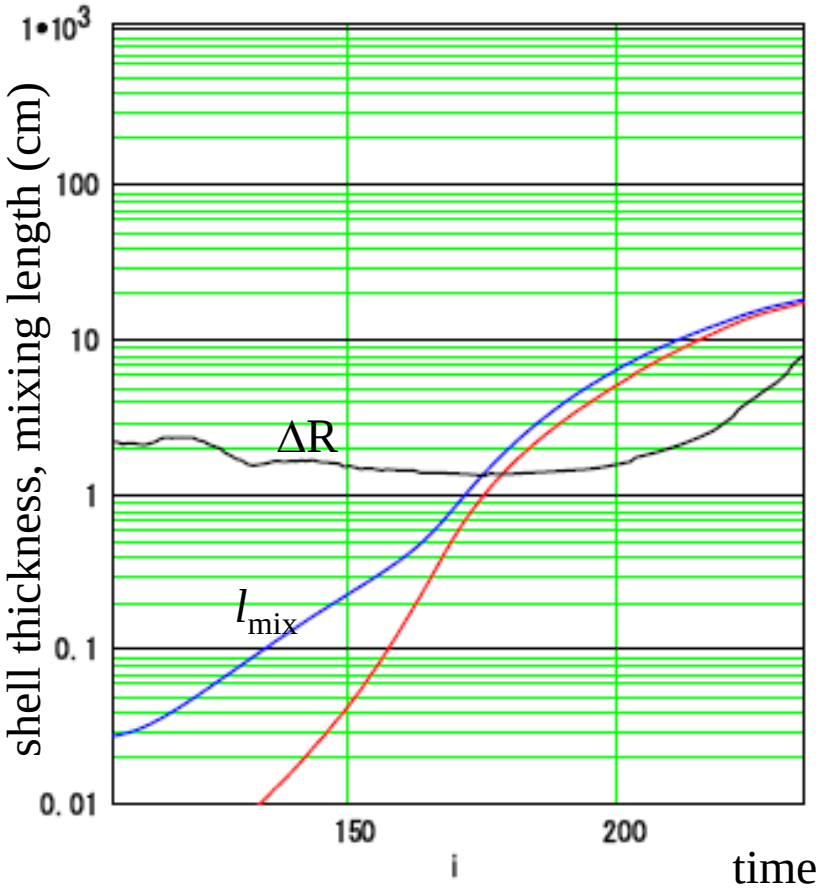

Detail 2-D rad-hydrodynamics simulations for fast ignition are performed to evaluate the implosion performance.

CD shell target ; multi-mode (l=2~40) , initial target surface perturbation is given in PINOCO-2D simulation

- target surface roughness
  measured + Nakai-Azechi initial imprint mode
- Uniform laser irradiation
- computational grid (310x352)

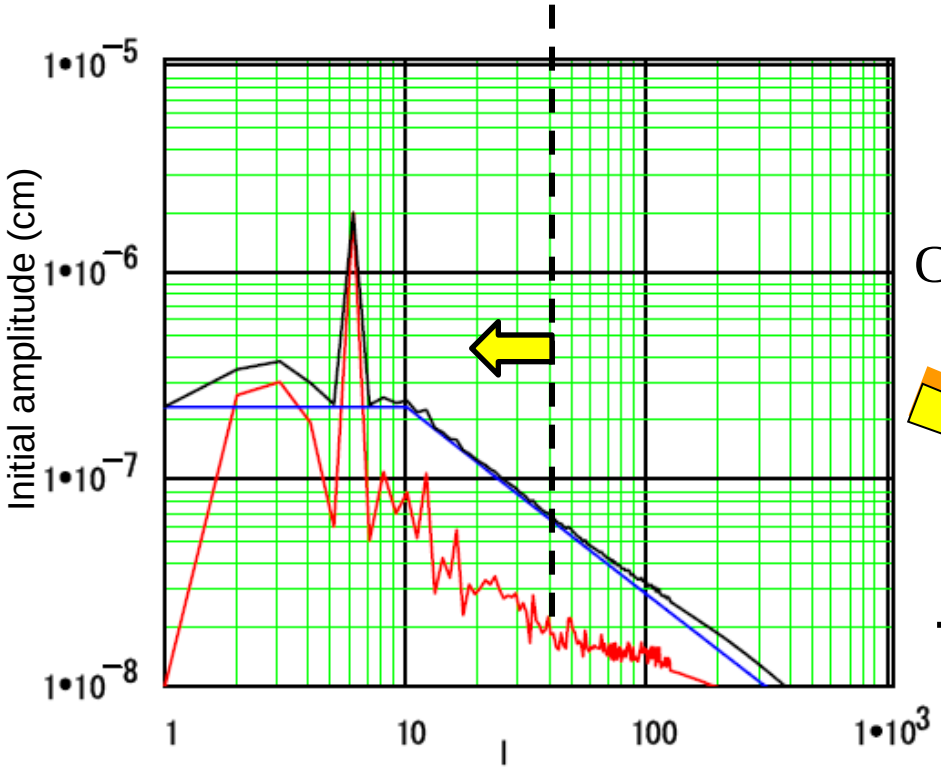

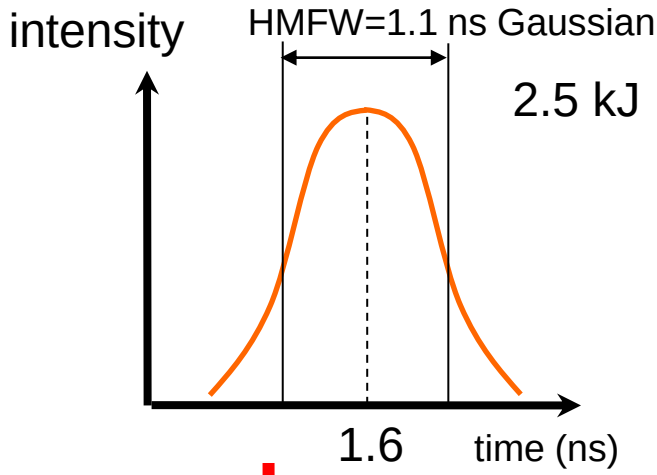

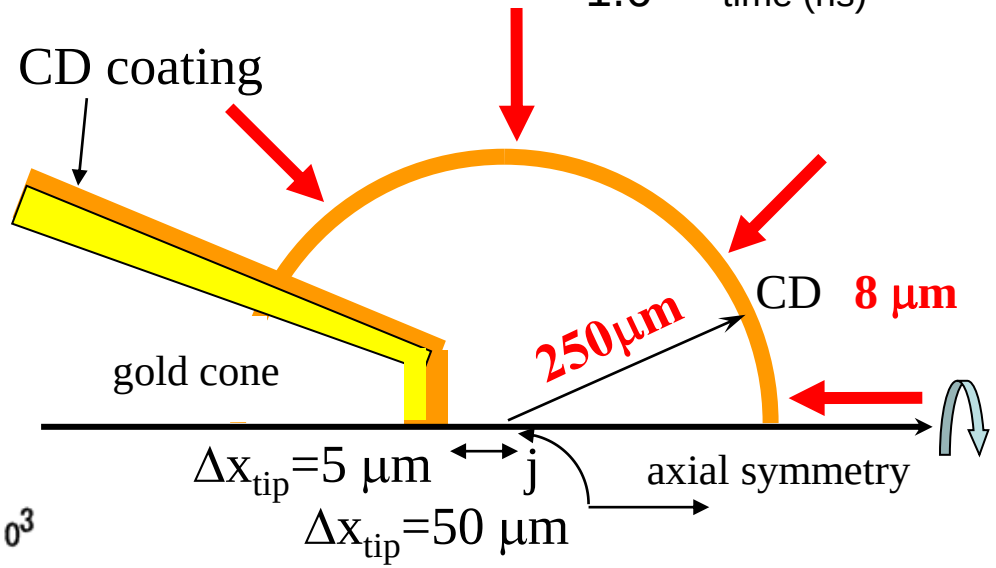

overview of the implosions (cone-guided without initial perturbation on the shell target surface) Yn=9.7x10^7

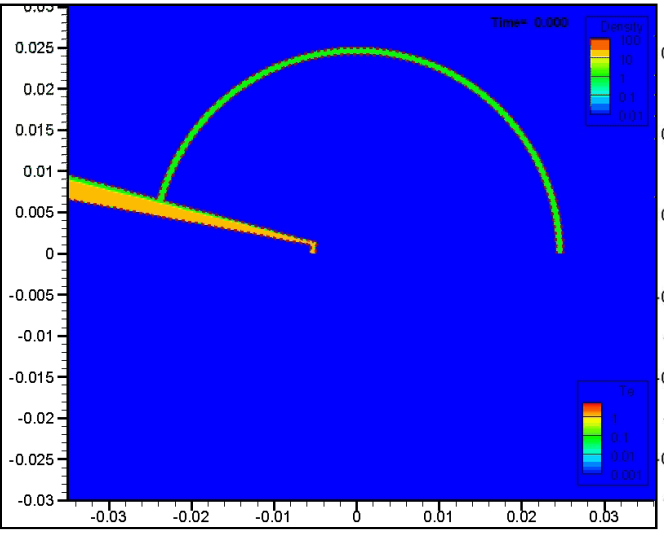

0.00 ns

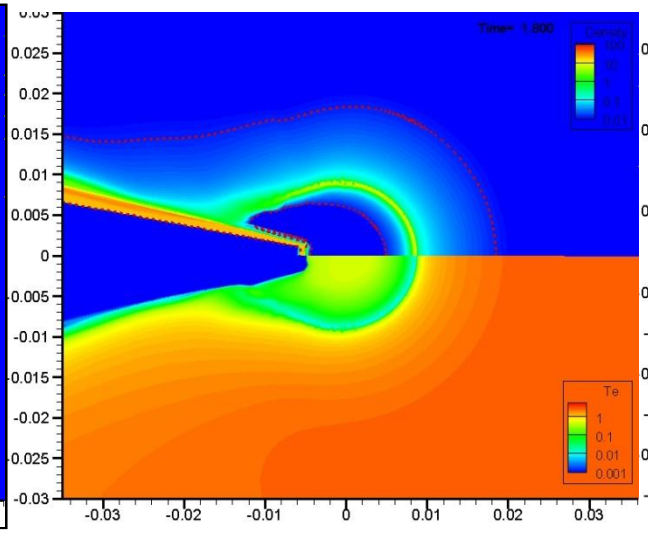

1.80 ns

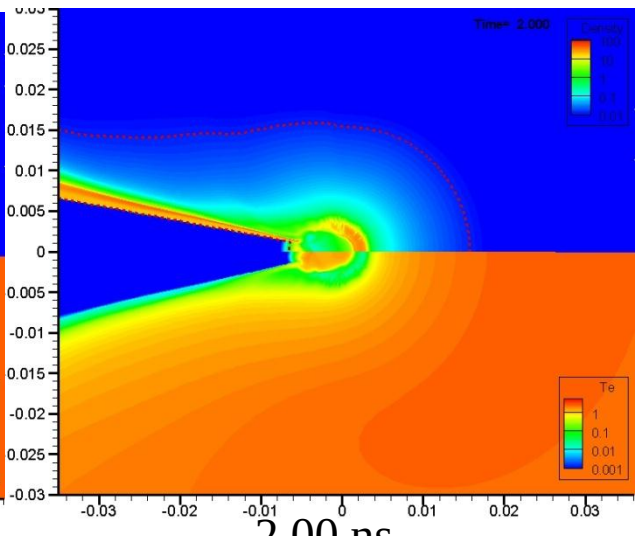

2.00 ns

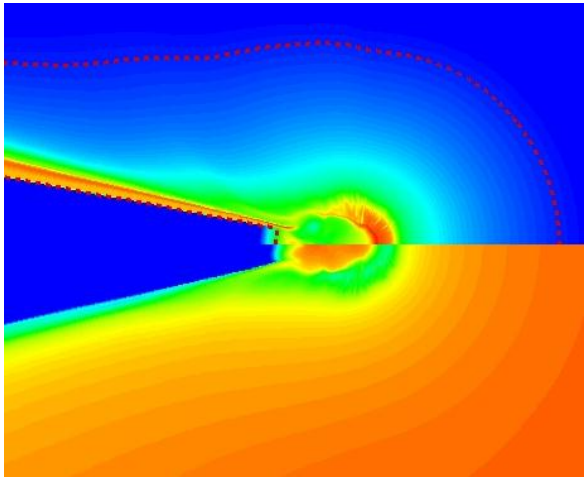

2.02 ns

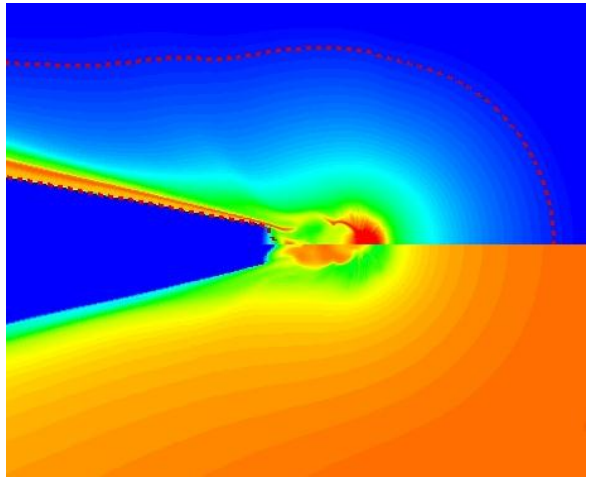

2.06 ns

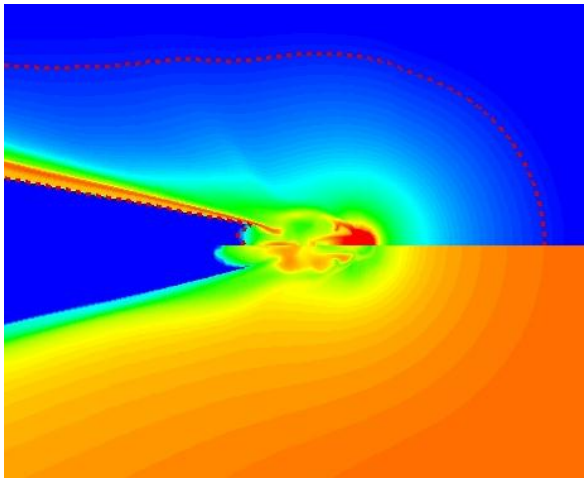

2.10 ns

overview of the implosions (cone-guided with initial perturbation on the shell target surface) Yn=5.9x10^{7}

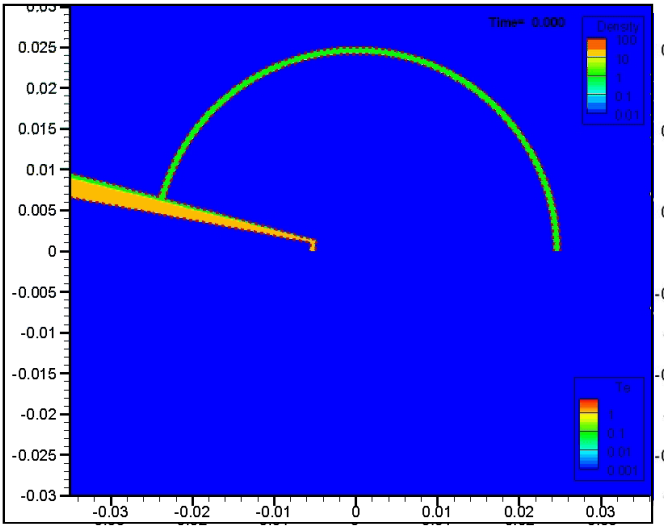

0.00 ns

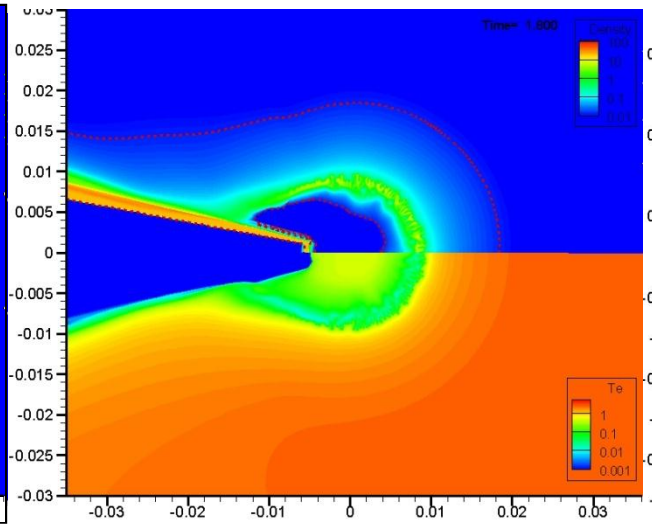

1.80 ns

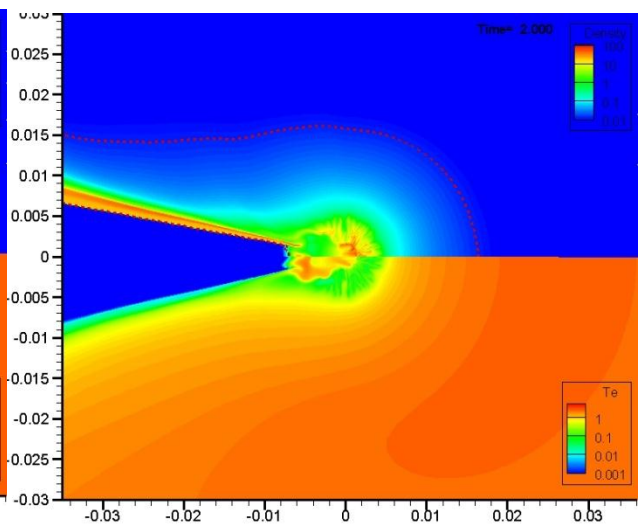

2.00 ns

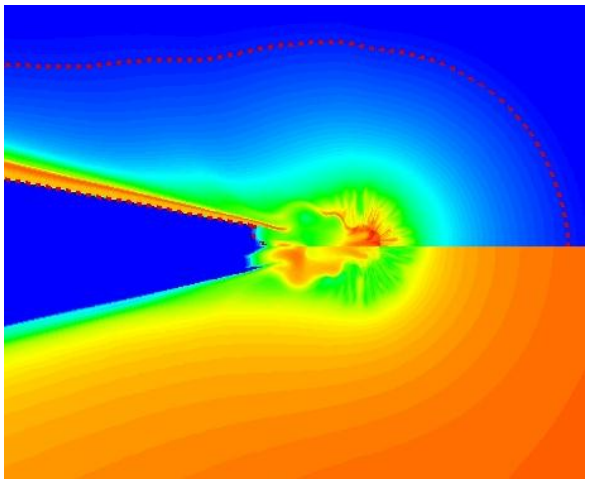

2.02 ns

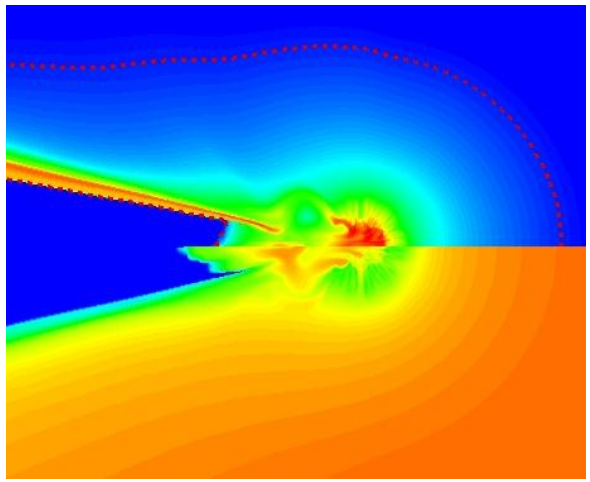

2.06 ns

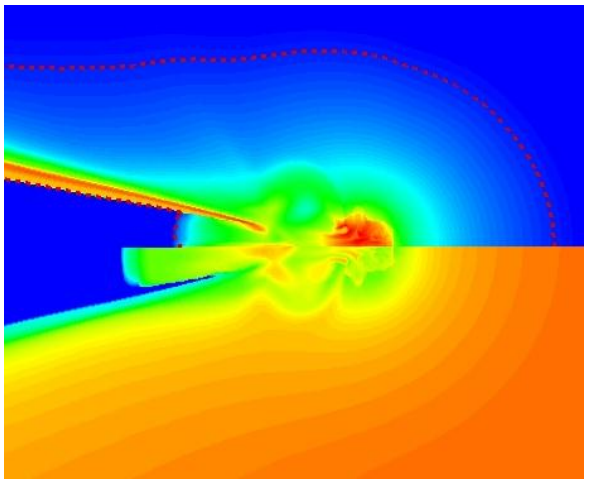

2.10 ns

ρR is reduced by the hydrodynamics instability

Angular dependence of ρR (average, minimum, maximum) are compared
(only quadrant spheres parts are evaluated)

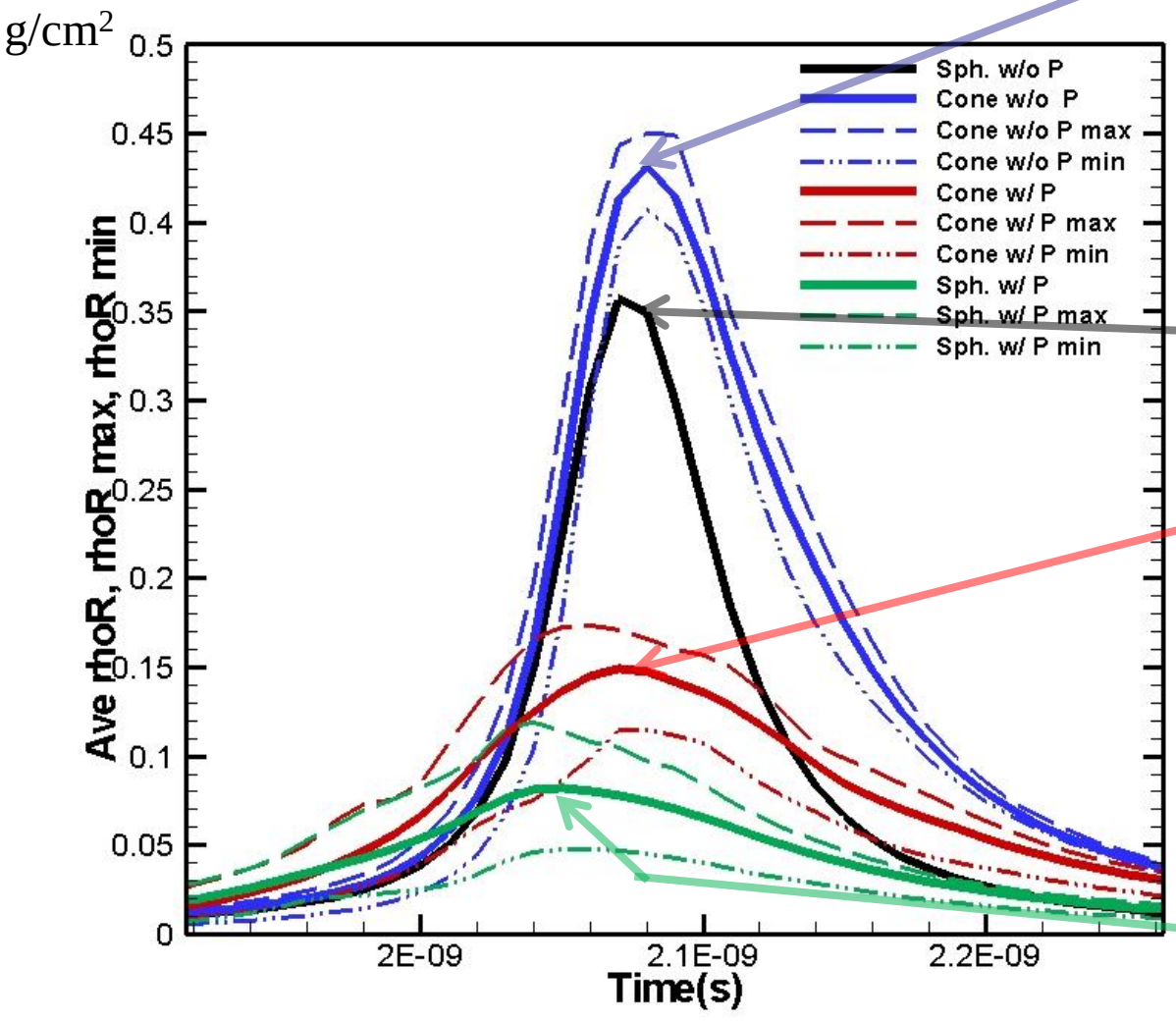

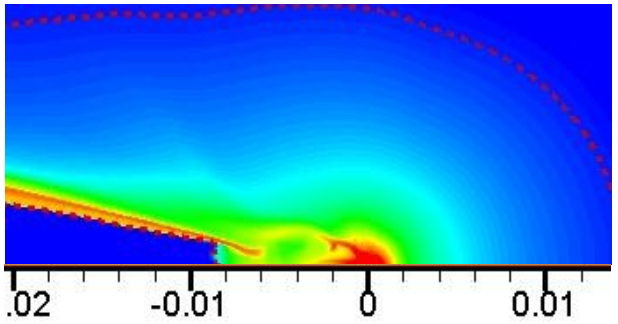

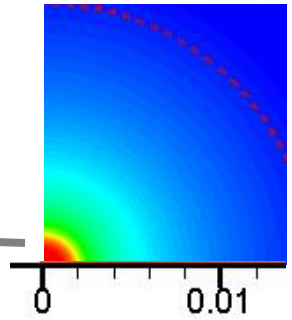

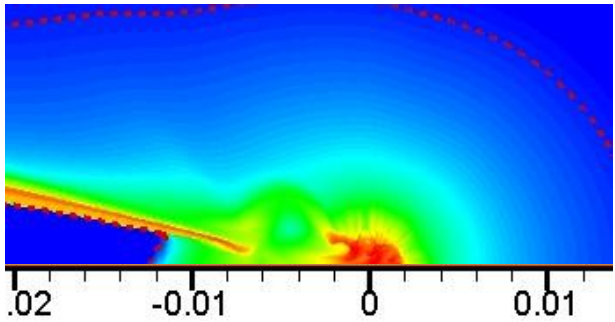

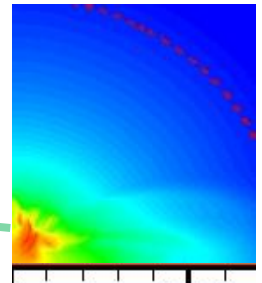

Cone tip is destroyed before the maximum compression time, if Rayleigh-Taylor instability is strongly grown.

During the imploding phase, due to the hydrodynamic instability which is occurred in acceleration phase, plasma expands into the shell, and the pressure inside the shell is increased.

Thus, the imploding shell is decelerated, and maximum mass density is dropped. Also, the inner plasma collides with the tip of the cone, and it is destroyed before the maximum compression time.

With initial perturbation

(t=1.97 ns, 100 ps before maximum compression, tip is broken.)

Yn=5.9x10^7

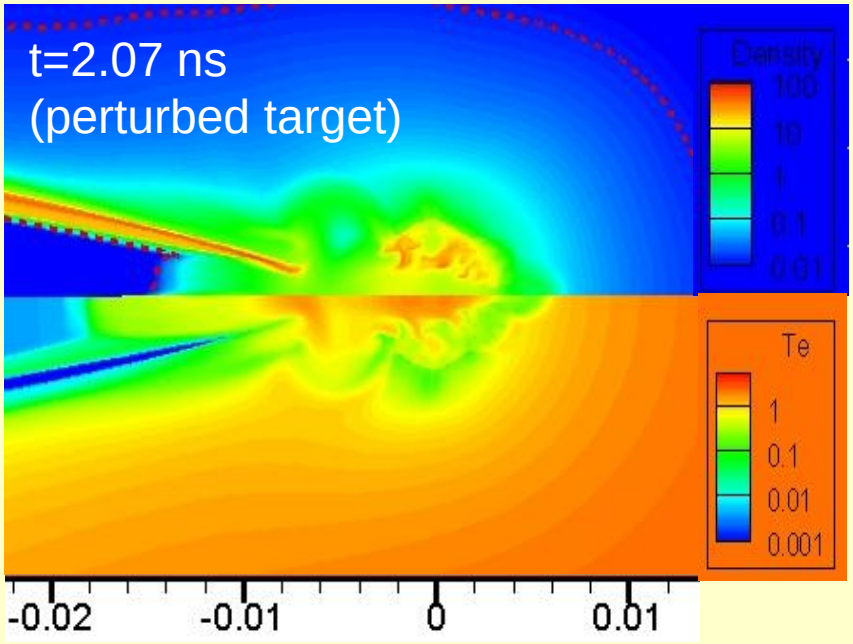

Without initial perturbation (clean cone-guided implosion)

Yn=9.7x10^7

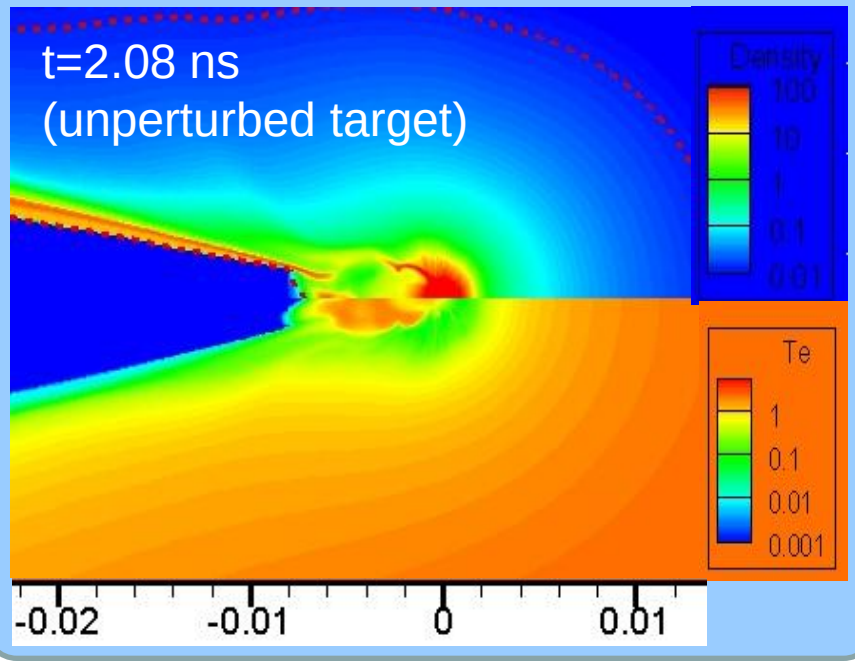

Slow implosion design FIREX-1.5

Target design using 1-D simulation

20kJ、0.35μm

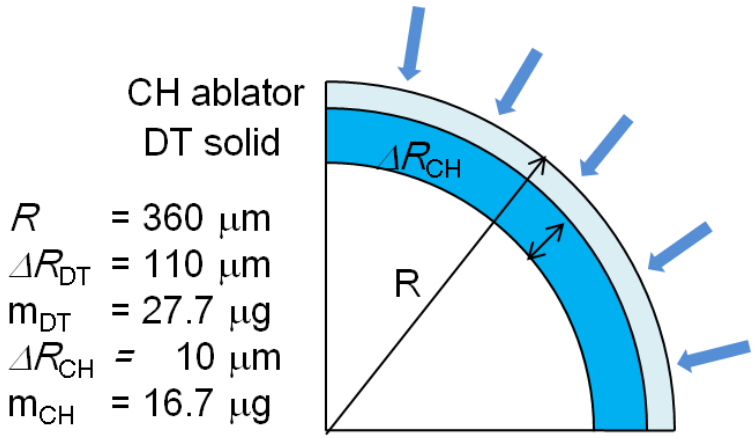

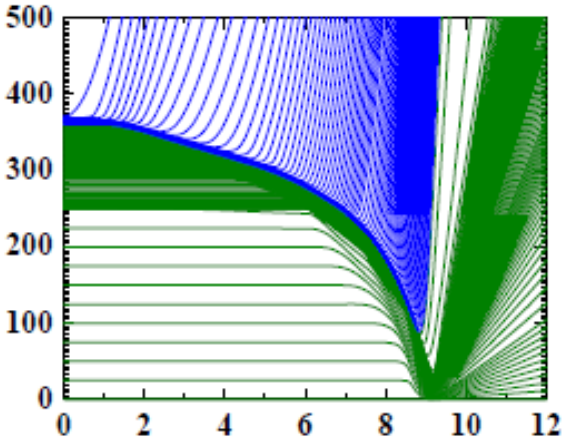

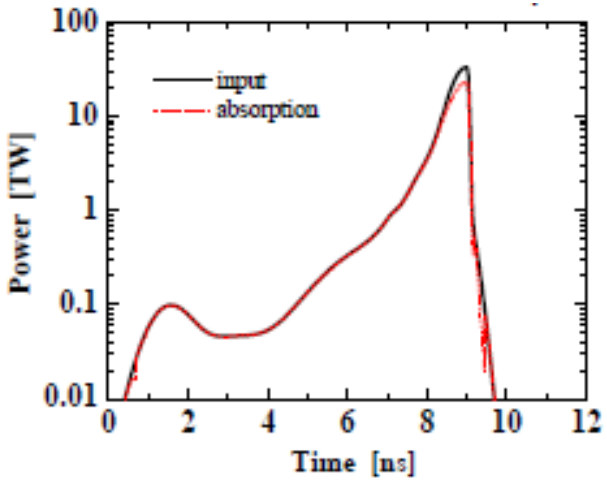

ρR_{DT} = 0.68g/cm^2 at t = 9.14ns
(maximum compression)

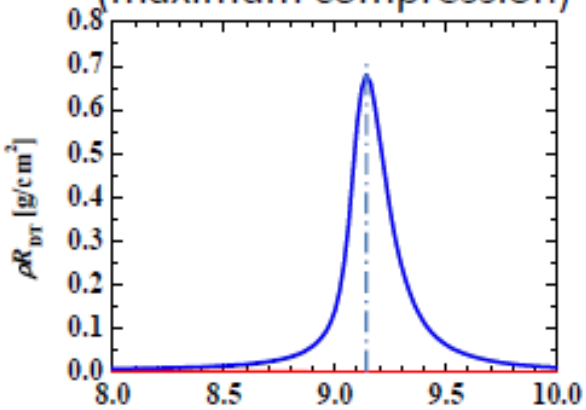

FI^3 Project

Fast Ignition Integrated Interconnecting code

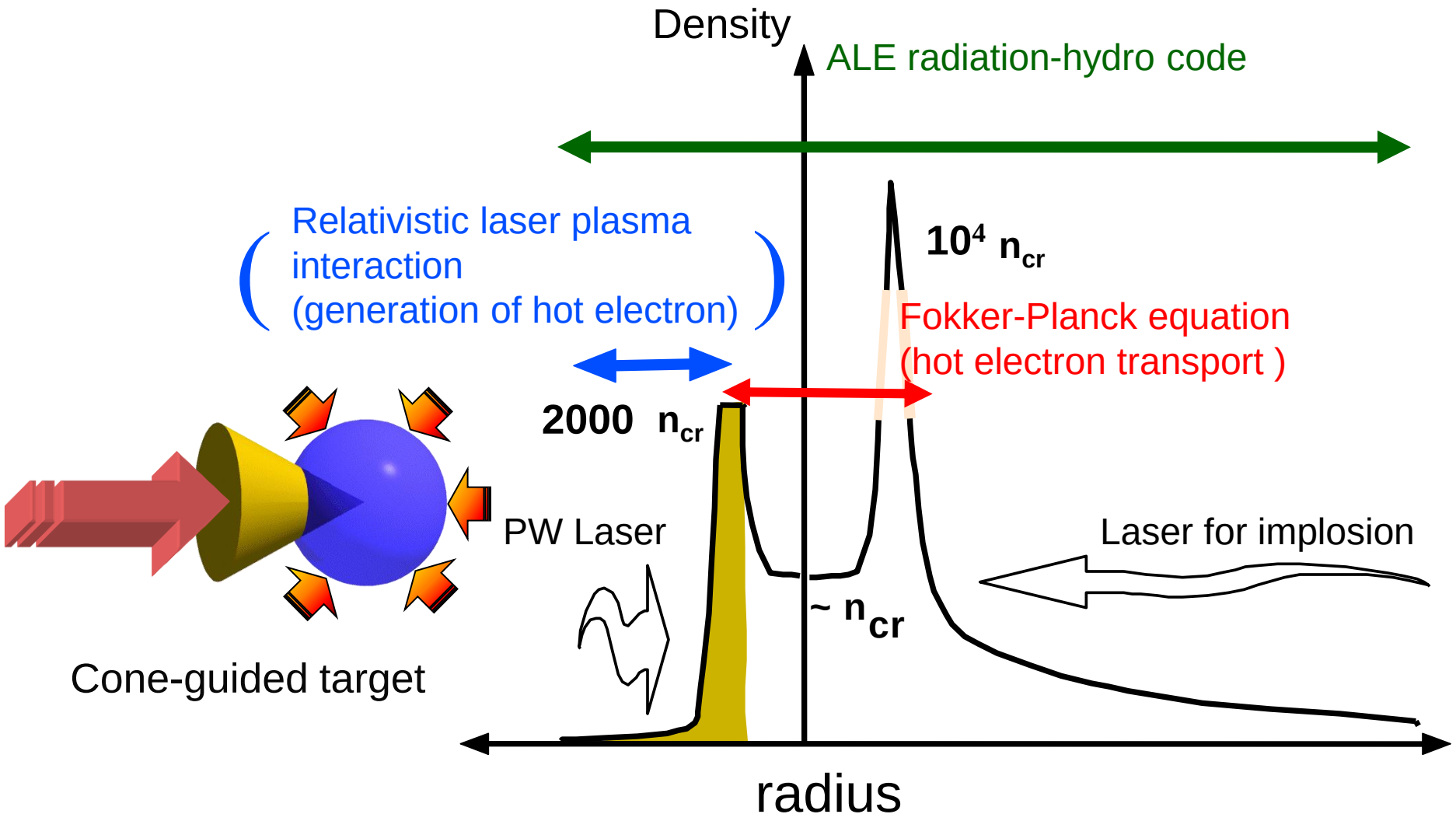

Integrated Simulations

FI^3 (Fast Ignition Integrated Interconnecting) Code System

Nagatomo, ILE

Radiation-Hydro "PINOCO"
(implosion)

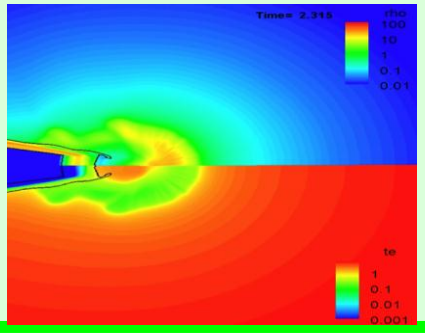

Sunahara, ILT

Radiation-Hydro "Star"
with 3D ray-trace & detailed atomic data
(pre-foamed plasma)

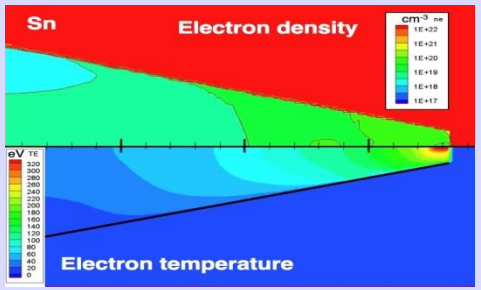

FI^3

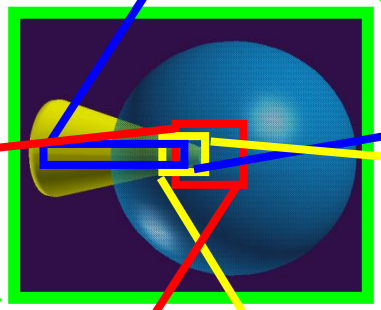

Imploded core & deformed cone profiles

Pre-formed plasma profile

FP-Hydro "FIBMET"
(core heating & fusion burning)

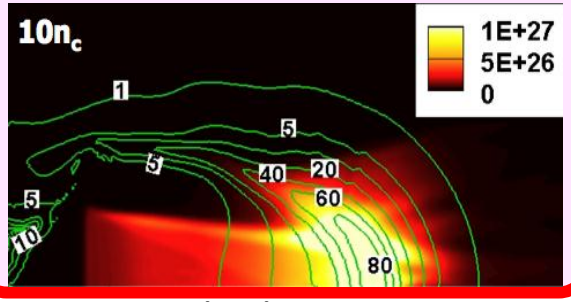

Johzaki, ILE

Fast electron & ion profiles

PIC "FISCOF"
(relativistic laser-plasma interaction)

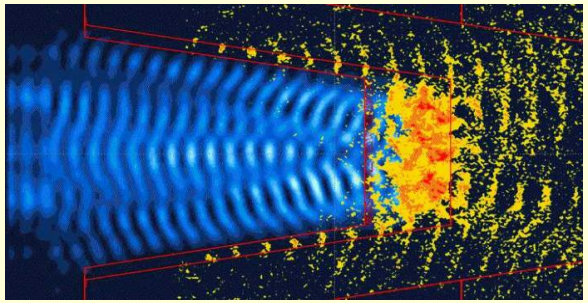

Sakagami, NIFS, Johzaki, ILE

FI^3 and DCCP

(Distributed Computing Collaboration Protocol)

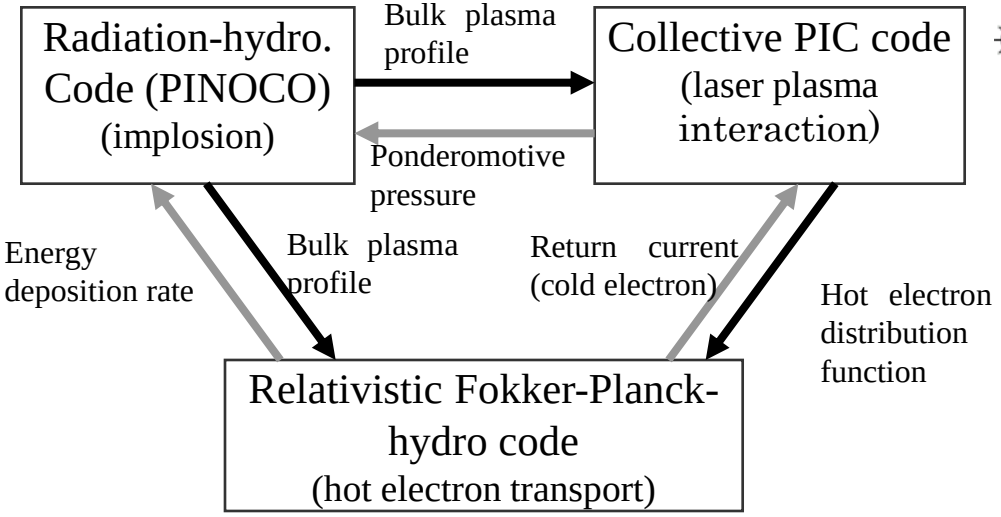

Data flow in FI^3 system. Black arrows are already executable data flows, and gray arrows are next plan to be considered.

- ☼ dynamic negotiation for communication pair
  - ○ Code can be invoked at an arbitrary computer.
- ☼ asynchronous communication
  - ○ Data will be automatically saved/restored.

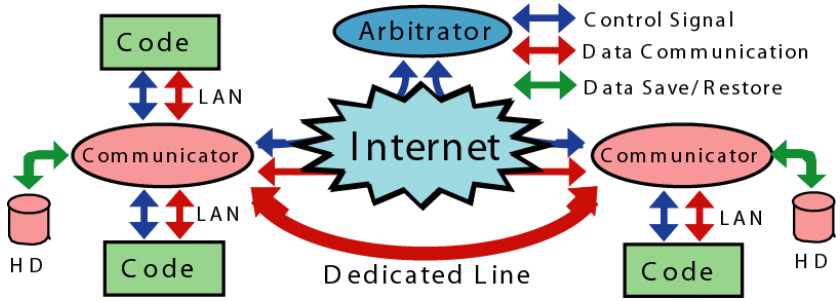

- ☺ Code (user' s simulation program)
  - does not transfer data directly to another code
- ☺ Communicator
  - receive data from sender code
  - forward data between different sites
  - send data to receiver code
- ☺ Arbitrator
  - manage information of codes
  - control data communication

H. Sakagami, NIFS